ECOLOGY

Inherent differential microbial assemblages and functions associated with corals exhibiting different thermal phenotypes

Erika P. Santoro[1,2]†, Anny Cárdenas[3,4]†, Helena D. M. Villela[1], Caren L. S. Vilela[2], Angela M. Ghizelini[2], Gustavo A. S. Duarte[1], Gabriela Perna[3], João P. Saraiva[5], Torsten Thomas[6], Christian R. Voolstra[3]*‡, Raquel S. Peixoto[1]*§

Certain coral individuals exhibit enhanced resistance to thermal bleaching, yet the specific microbial assemblages and their roles in these phenotypes remain unclear. We compared the microbial communities of thermal bleaching–resistant (TBR) and thermal bleaching–sensitive (TBS) corals using metabarcoding and metagenomics. Our multidomain approach revealed stable distinct microbial compositions between thermal phenotypes. Notably, TBR corals were inherently enriched with microbial eukaryotes, particularly Symbiodiniaceae, linked to photosynthesis, and the biosynthesis of antibiotic and antitumor compounds and glycosylphosphatidylinositol-anchor proteins, crucial for cell wall regulation and metabolite exchange. In contrast, TBS corals were dominated by bacterial metabolic genes related to nitrogen, amino acid, and lipid metabolism. The inherent microbiome differences between TBR and TBS corals, already observed before thermal stress, point to distinct holobiont phenotypes associated to thermal bleaching resistance, offering insights into mechanisms underlying coral response to climate-induced stress.

INTRODUCTION

Corals are foundational species that support reef ecosystems, which provide habitat for more than a third of marine life (*1*). These ecologically and economically important ecosystems are threatened by local and/or global stressors (*2*), such as pollution (*3*) and ocean warming (*4*). Coral bleaching (i.e., the disruption of the relationship between the host and the endosymbiont photosynthetic algae from the family Symbiodiniaceae), mainly caused by ocean warming, has been considered one of the main drivers of the massive die-offs in different regions in the past decades (*5*, *6*).

Despite their general sensitivity to thermal stress, some coral populations (*7*, *8*) and individuals (*8*–*10*) demonstrate differential susceptibility to thermal bleaching. Although there is no consensus in the literature on the use of the terms thermal "resistance," "tolerance," or "sensitivity" for corals or other marine organisms, here, we consider corals that retain their pigmentation during a bleaching event as bleaching resistant corals, as recently suggested by Matsuda *et al.* (*10*). Resistant phenotypes can occur through adaptation or acclimatization of the different members of the holobiont. By definition, adaptation consists of a process that occurs over generation(s), helping individuals and populations to permanently increase their fitness (*11*). Acclimatization, in contrast, refers to physiological plasticity that allows a single individual to be temporally and reversibly more tolerant or resistant to a specific condition (*12*). These processes can be linked to the coral host, the photosynthetic endosymbiotic algae of the Symbiodiniaceae family, and the other members of the coral microbiome, each of them potentially playing a role in resistance mechanisms (*13*). Some studies attributed coral resistance to host adaptation via natural selection of a heat-resistant state due to exposure to, for example, naturally warmer temperature regimes (*7*, *14*). This process can be induced by exposure to subbleaching temperatures (*15*, *16*) and/or to associations with beneficial microbial assemblages [either Symbiodiniaceae (*17*, *18*) or bacterial communities (*19*, *20*)]. For example, specific associations between corals and some members of the Symbiodiniaceae family, such as those of the genus *Durusdinium*, have been demonstrated to contribute to differences in heat tolerance (*21*). Other members of the microbial community may be an even more plastic and dynamic part of the holobiont and could contribute to physiological improvements on a much more flexible or shorter timescale than genetic adaptations of the host (*22*) or changes in the Symbiodiniaceae populations (*23*). The role of microbial groups other than the photosynthetic algae, such as bacteria or viruses, has been explored in coral fitness and thermal stress resistance (*19*, *24*, *25*). For example, some specific bacteria can quickly respond to environmental impacts (*22*, *26*) and contribute to the holobiont's increased resistance to heat stress (*27*, *28*), although the ability to change microbial association (i.e., microbial flexibility) differs between host species (*22*, *29*).

Despite the interconnections between all members of the holobiont and their potential links to coral resistance, most studies have focused on either host-Symbiodiniaceae (*23*) or host-bacteria (*19*) associations, with some recent insights into the microbiome associated with cultures of free-living (*30*) and in hospite Symbiodiniaceae (*31*), or the role of the microbiome in modulating the host's epigenome (*32*). Specific holistic and multidomain assemblages and potential mechanisms associated with corals exhibiting differential thermal bleaching susceptibility and its response to thermal stress

[1]Division of Biological and Environmental Science and Engineering (BESE), King Abdullah University of Science and Technology (KAUST), Thuwal, Saudi Arabia. [2]IMPPG, Federal University of Rio de Janeiro, Rio de Janeiro, Brazil. [3]Department of Biology, University of Konstanz, Konstanz, Germany. [4]Department of Biology, American University, Washington, D.C. 20016, USA. [5]Department of Environmental Microbiology, Helmholtz Center for Environmental Research – UFZ, Leipzig, Germany. [6]Center for Marine Science and Innovation, School of Biological, Earth and Environmental Sciences, University of New South Wales, Sydney, Australia.
*Corresponding author. Email: raquel.peixoto@kaust.edu.sa (R.S.P.); christian.voolstra@uni-konstanz.de (C.R.V.)
†These authors contributed equally to this work.
‡Present address: Department of Biology, University of Konstanz, Konstanz, Germany.
§Present address: Marine Microbiomes Laboratory, Red Sea Research Center (RSRC), King Abdullah University of Science and Technology (KAUST), Thuwal 23955-6900, Kingdom of Saudi Arabia.

have not yet been fully explored. Given the rapid pace of current environmental changes, elucidating the mechanisms and taxa underlying coral health (*25*, *33*) and bleaching resistance in coral holobionts is crucial for developing strategies to boost coral resilience and reduce mortality under future climate change scenarios (*34*–*37*).

Here, we examine two phenotypes of the same coral species (*Mussismilia hispida*) exhibiting different levels of resistance to bleaching that were categorized into thermal bleaching resistant (TBR) and thermal bleaching sensitive (TBS) based on their differential responses to heat stress during long-term experiments. Our results reveal that each phenotype inherently harbors specific microbial assemblages and each group contributes proportionally differently to the holobiont's metabolic traits. Furthermore, TBR corals exhibited a higher abundance of microbial eukaryotes, predominantly Symbiodiniaceae, influencing their metabolic profiles, particularly photosynthetic and membrane anchoring proteins, as well as the biosynthesis of antibiotic and antitumor compounds. In contrast, bacteria was the main group contributing to metabolic genes associated with TBS corals, including nitrogen, amino acid, and lipid metabolism. While shifts in the microbial structure were observed in response to heat stress over time within each phenotype, no overall changes were detected in the functional profiles of either TBR or TBS, suggesting that inherent stable differences may contribute to distinct thermal resistance. These findings indicate a correlation between the coral-Symbiodiniaceae-microbiome assembly, providing key insights to inform strategies aiming to counteract coral mortality in the face of climate change.

RESULTS

Different *M. hispida* phenotypes exhibit distinct bleaching responses during thermal stress experiments

Pilot heat stress experiments were conducted previously to test colonies obtained from a collection of the Marine Aquarium of Rio de Janeiro (AquaRio), in which it was observed that some colonies bleached at 30.5°C (tagged as TBS) and others did not exhibit signs of visual bleaching at this temperature (tagged as TBR) (see Supplementary Material and Methods). These initial experiments guided the design of the heat stress experiments (Fig. 1A) to investigate specific shifts in microbial groups associated with each phenotype. Four colonies from each of the TBR and TBS phenotypes were selected based on the pilot experiment. Two parallel long-term mesocosm experiments (Fig. 1A) were conducted to explore the thermal bleaching susceptibility of TBR and TBS and to investigate shifts in the microbiome associated with each phenotype. Fragments of each phenotype were exposed to a pre-peak temperature (29.5°C for TBS and 30.5°C for TBR) for 10 days, followed by 4 days at peak temperature (30.5°C for TBS and 32°C for TBR) and a recovery period of 15 days at 26°C.

The two phenotypes of *M. hispida* displayed different responses under increasing temperature regimes. Bleaching scoring was performed using the Coral Health Chart as a reference (*38*). TBS fragments bleached immediately after the heat stress peak (T1) at 30.5°C, with all replicates decreasing at least two units on the Coral Health Chart after heat stress when compared to their score at T0. After 3 days of recovery at 26°C, one of the TBS replicas died, and, at the end of the experiment, the remaining fragments remained severely bleached (fig. S1). In contrast, the color of TBR fragments only decreased by one unit after the heat stress peak (T1) at 32°C (fig. S1) when compared to T0, exhibiting no visual signs of bleaching or tissue damage throughout the experiment, even when exposed to higher temperatures than the TBS corals.

The applied thermal stress also differently affected the photosynthetic performance of the associated symbiotic algae, as evaluated by F_v/F_m measurements (Fig. 1, B and C, respectively). TBR corals exhibited a modest decrease of 15% in their F_v/F_m values from T0 to T1, which was found to be statistically significant compared to the values at T0 [$P = 0.016$, effect size $d = -3.08$; 95% confidence interval (CI) = (−7.85, −1.69)]. However, no significant differences were observed at T2 when compared to T0 [$P = 0.79$, effect size $d = -2.15$; 95% CI = (−4.81 −0.51)], indicating that TBR endosymbiotic algae were able to recover their photosynthetic efficiency. Although TBS corals exhibited a notable 29% decrease in their F_v/F_m values from T0 to T1, this change was not found to be statistically significant (t ratio = −1.809, $P = 0.12$). However, a significant decrease was observed at T2 when compared to T0 [t ratio = 4.251, $P = 0.016$, effect size $d = -2.59$; 95% CI = (−6.22, −1.04); table S1]. The differential response of TBR and TBS corals to the applied heat stress demonstrates a clear phenotypic difference. Next, we investigated how the microbiome of these two different phenotypes are organized and may functionally support the differential thermal resistance.

Corals with distinct thermal resistance inherently harbor distinct microbiome assemblages

TBR and TBS coral phenotypes are associated with distinct Symbiodiniaceae assemblages

To evaluate inherent differences between microbial assemblages associated with corals that exhibit distinct levels of thermal resistance, we first assessed differences in Symbiodiniaceae composition at T0. Internal transcribed spacer 2 (ITS2) amplicon sequencing of TBR ($n = 3$) and TBS coral ($n = 3$) samples revealed that each phenotype was associated with significantly different algal assemblages [permutational multivariate analysis of variance (PERMANOVA): $P = 0.001$, $R^2 = 0.77$; table S2 and Fig. 2A]. The most abundant Symbiodiniaceae lineage harbored by TBR corals was *Symbiodinium* ITS-type A4 (62% mean ± 0.54 SD) followed by a low portion of *Cladocopium* C21-C3vv-C3-C3vw-C50br (5% mean ± 0.005 SD). Notably, one of the replicates of TBR samples (E23) appears as an outlier, as A1/A4-A1b (94% relative abundance) was the most abundant lineage in all the other samples. In contrast, TBS corals were dominated by *Cladocopium* C3-C3vv-C3ww-C3-C50br-C3vu (86% mean ± 0.016 SD), followed by a low portion of *Symbiodinium* ITS-typing A4/A1-A4br-A4bq-A1mi-A1b (13% mean ± 0.016 SD), as shown in Fig. 2B.

Distinct microbial associations in corals with different thermal phenotypes

In addition to the characterization of Symbiodiniaceae assemblages, we investigated other microbial groups associated with the different coral phenotypes before the heat stress (T0). For this purpose, metagenomic shotgun sequencing and 16*S* ribosomal RNA (rRNA) gene amplicon sequencing were conducted to evaluate the microbial diversity associated with TBR and TBS corals.

A total of 1,931,790 open reading frames (ORFs) were identified from the metagenomic data, of which 709,392 were taxonomically classified by Kaiju to at least the domain level, and 1628 (37%) were classified at the family level. The biodiversity analysis revealed significant overall differences in Shannon alpha diversity [analysis of variance (ANOVA) $P < 0.001$, Eta-squared ($\eta 2$) = 0.93; Fig. 3A and table S3] and beta diversity (PERMANOVA $P = 0.001$, $R^2 = 0.44$; Fig. 3B and table S3) of metagenomic families between phenotypes. In addition, analysis of microbiome compositions with bias correction (ANCOM-BC) was performed to estimate differentially abundant

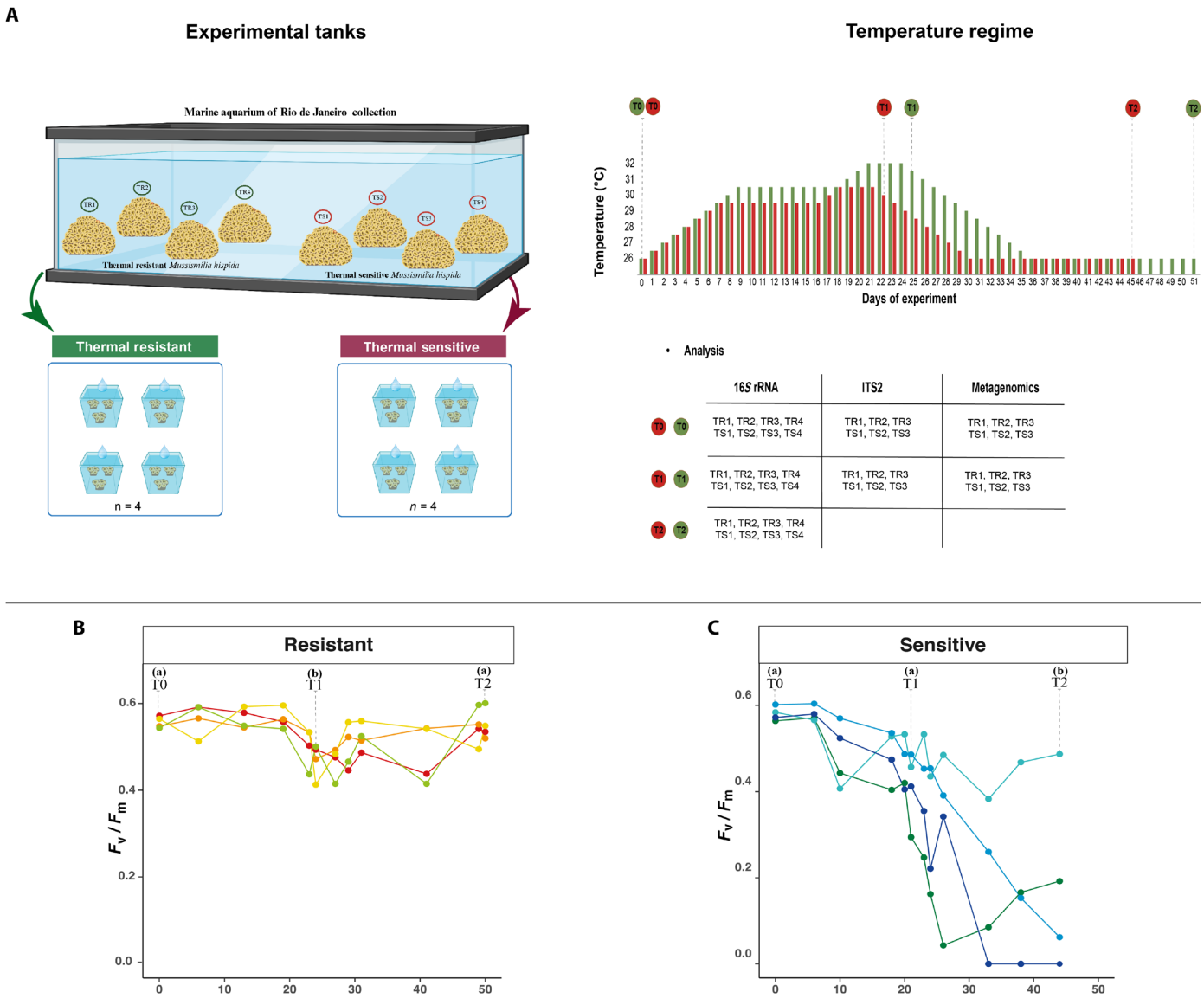

Fig. 1. Experimental design and *Fv/Fm* rates of Thermal Bleaching Resistant (TBR) and Thermal Bleaching Sensitive (TBS) coral phenotypes. (**A**) Experimental design using corals exhibiting TBR and TBS phenotypes. Temperature regime and means of the photosynthetic efficiency (F_v/F_m) ratios (*y* axis) throughout the experiment (*x* axis, days of the experiment) of TBR (**B**) and TBS (**C**) corals. The F_v/F_m values corresponding to the sampling times were measured the night before sampling. The same letters mean no significant differences, while different letters mean significant differences ($P < 0.05$) when compared to the beginning of the experiment (T0). The F_v/F_m values correspond to the same fragment throughout the experiment.

(DA) taxa between metagenomic data from different groups, in which TBR corals were enriched with microbial eukaryotes when compared with TBS [ANCOM-BC–log folder change (LFC) = 1.31, W = 7.99, $P < 0.001$; table S4]. The most notable difference in microbial eukaryotes composition was the significantly higher abundance of Symbiodiniaceae in TBR (89.42% of the total community, ±1.74 SD) compared to the TBS (68.36% of the total community, ±2.71 SD) phenotype (fig. S2). The different phenotypes were intricately associated with distinct microbial assemblages across all domains. A total of 289 metagenomic families were differentially abundant between phenotypes (table S5). Metagenomic families Brevinemataceae (ANCOM-BC–LFC = 5.7, W = 25.24, $P < 0.001$), Thiofilaceae (ANCOM-BC–LFC = 5.68, W = 14.62, $P < 0.001$), Amoebophilaceae (ANCOM-BC–LFC = 4.49, W = 11.10, $P < 0.001$), and Rhabdochlamydiaceae (ANCOM-BC–LFC = 3.85, W = 6.21, $P < 0.001$) were among the most enriched bacteria in TBR. Pithophoraceae (ANCOM-BC–LFC = 5.57, W = 13.22, $P < 0.001$), Siphonocladaceae (ANCOM-BC–LFC = 5.55, W = 13.39, $P < 0.001$), and Dinophysiacea (ANCOM-BC–LFC = 4.4, W = 8.95, $P < 0.001$) were the TBR top-enriched eukaryotes, while the most TBR-abundant viruses were represented by Caulimoviridae (ANCOM-BC–LFC = 3.35, W = 9.09, $P < 0.001$), Leviviridae (ANCOM-BC–LFC = 2.84, W = 7.67, $P < 0.001$), and Hepadnaviridae (ANCOM-BC–LFC = 2.57, W = 7.03, $P < 0.001$). Last, the most enriched Archaea in TBS were Methanospirillaceae (ANCOM-BC–LFC = 2.69, W = 7.61, $P < 0.001$), Caldisphaeraceae (ANCOM-BC–LFC = 2.38, W = 6.58, $P = 0.001$), and

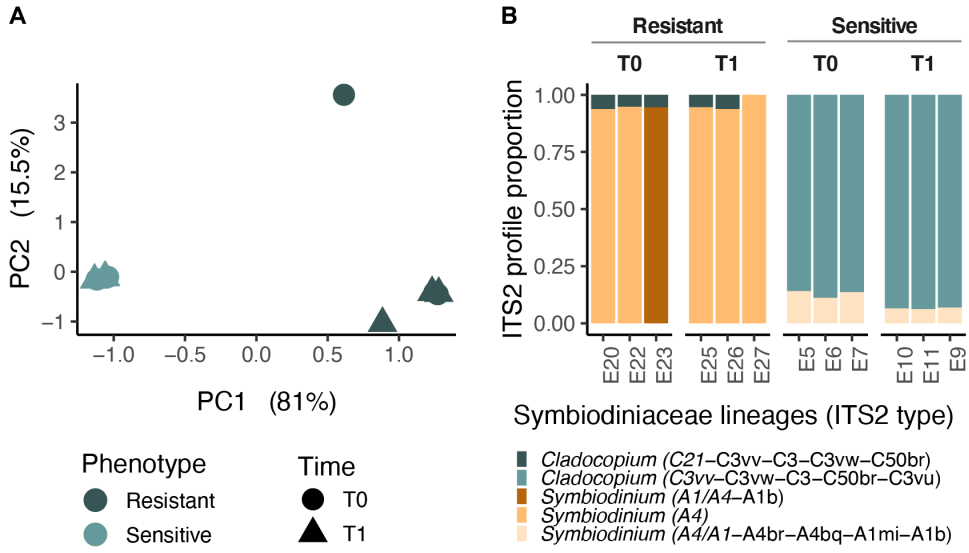

Fig. 2. Symbiodiniaceae assemblages associated with TBR and TBS coral phenotypes. (**A**) Principal components analysis plot of *Symbiodiniaceae* assemblage (ITS2 types) in TBR and TBS corals; (**B**) *Symbiodiniaceae* lineages distribution (ITS2 type) in TBR and TBS corals.

Nitrososphaeraceae (ANCOM-BC–LFC = 2.33, W = 6.44, $P < 0.001$) (Fig. 3C and table S5).

TBS corals were mainly enriched with Celerinatantimonadaceae (ANCOM-BC–LFC = 3.55, W = 16.48, $P < 0.001$), Pasteuriaceae (ANCOM-BC–LFC = 2.58, W = 10.96, $P < 0.001$), Patulibacteraceae (ANCOM-BC–LFC = 245, W = 10.45, $P < 0.001$), and Vallitaleaceae (ANCOM-BC–LFC = 2.45, W = 7.71, $P < 0.001$) metagenomic bacterial families, whereas Tribonemataceae (ANCOM-BC–LFC = 4.38, W = 14.33, $P = 0.005$), Lophiotremataceae (ANCOM-BC–LFC = 2.72, W = 12.04, $P < 0.001$), and Delitschiaceae (ANCOM-BC–LFC = 2.57, W = 12.78, $P < 0.001$) were some of the enriched TBS eukaryotic families. The archaea Thermococcaceae (ANCOM-BC–LFC = 1.33, W = 5.80, $P < 0.001$) and viruses Totiviridae (ANCOM-BC–LFC = 2.0, W = 7.28, $P = 0.002$), Orthomyxoviridae (ANCOM-BC–LFC = 1.83, W = 5.21, $P = 0.001$), and Adenoviridae (ANCOM-BC–LFC = 1.77, W = 4.60, $P = 0.002$) were also correlated with TBS (Fig. 3C and table S5).

To further explore the bacterial communities of TBR and TBS corals at a higher resolution, 16*S* rRNA gene amplicon libraries of T0 samples were also sequenced. After removing potential kit contaminants and amplicon sequence variants (ASVs) classified as mitochondria and chloroplasts, 2660 ASVs were retained for downstream analysis. Inherent differences in the diversity and composition of the bacterial community between TBR and TBS corals were also evident through 16*S* rRNA gene amplicon sequencing data. Alpha (Shannon index–ANOVA, $P = 0.005$, Eta-squared (η2) = 0.307; Fig. 3D and table S6) and beta (PERMANOVA, $P = 0.001$, $R^2 = 0.13$; Fig. 3E and table S6) diversity data were significantly different between the coral phenotypes before any stress was applied. A total of 44 genera were found to be differentially abundant between TBR and TBS, also demonstrating distinct assemblages in the bacterial compartment (table S7). Genera mainly belonging to Alphaproteobacteria but also from Verrucomicrobiae, Clostridia, Spirochaetales, Cytophagales, Phycisphaerales, and Oligoflexia were enriched in TBR corals, in which the most interesting are Rhizobiales (ANCOM-BC–LFC = 3.25, W = 12.18, $P < 0.001$ and LFC = 1.71, W = 5.85, $P < 0.001$), Clostridia (ANCOM-BC–LFC = 2.06, W = 4.38, $P = 0.002$), *Paramaledivibacter* (ANCOM-BC–LFC = 3.10, W = 6.42, $P < 0.001$), Cytophagales (ANCOM-BC–LFC = 3.03, W = 7.76, $P < 0.001$), *Spirochaeta* (ANCOM-BC–LFC = 1.68, W = 6.11, $P < 0.001$), and *Sphingorhabdus* (ANCOM-BC–LFC = 1.61, W = 6.70, $P < 0.001$) (Fig. 3F and table S7). In contrast, genera belonging to the Verrucomicrobiota, Alphaproteobacteria, Gammaproteobacteria, Polyangia, Planctomycetota, Cyanobacteria, Bdellovibrionia, and Acidimicrobiia classes were enriched in TBS corals, in which *Roseovarius* (ANCOM-BC– LFC = 1.51, W = 6.94, $P < 0.001$) and an unknown genus of the Rhodobacteraceae family (ANCOM-BC– LFC = 1.10, W = 3.34, $P = 0.003$), *Waddlia* (ANCOM-BC–LFC = 3.0, W = 8.51, $P = 0.003$), an unknown genus of the Rickettsiales order (ANCOM-BC–LFC = 2.6, W = 6.15, $P < 0.001$), *Agaribacterium* (ANCOM-BC–LFC = 1.97, W = 7.06, $P < 0.001$), and Gammaproteobacteria D90 (ANCOM-BC–LFC = 2.0, W = 7.87, $P < 0.001$) are among them (Fig. 3F and table S7).

Distinct functional profiles in corals with different thermal phenotypes

To further understand the functional profiles underlying the observed differences in thermal resistance, we investigated the metagenomic functions associated with TBR and TBS assemblages at T0. A total of 17,617 Kyoto Encyclopedia of Genes and Genomes (KEGG) orthologs (KOs) were identified in the metagenomic samples. The functional profiles of TBR and TBS phenotypes were significantly different from each other (PERMANOVA, $P = 0.003$, $R^2 = 0.3$; Fig. 4A and table S8), with 3120 distinct genes differentially enriched (ANCOM-BC test) in each phenotype (table S9). Overall, metabolic KOs seem to mark the most notable difference between TBR and TBS (Fig. 4B). In addition, the number of differentially abundant metabolic KOs belonging to each microbial group was proportionally different within TBR and TBS corals, with TBR corals having more metabolic KOs from microbial eukaryotes, whereas most of the metabolic KOs in TBS are from bacteria (Fig. 4C). Metabolic KOs, particularly those involved in protein metabolism (137 DAs) from microbial eukaryotes in TBR corals, exhibit notable enrichment, alongside

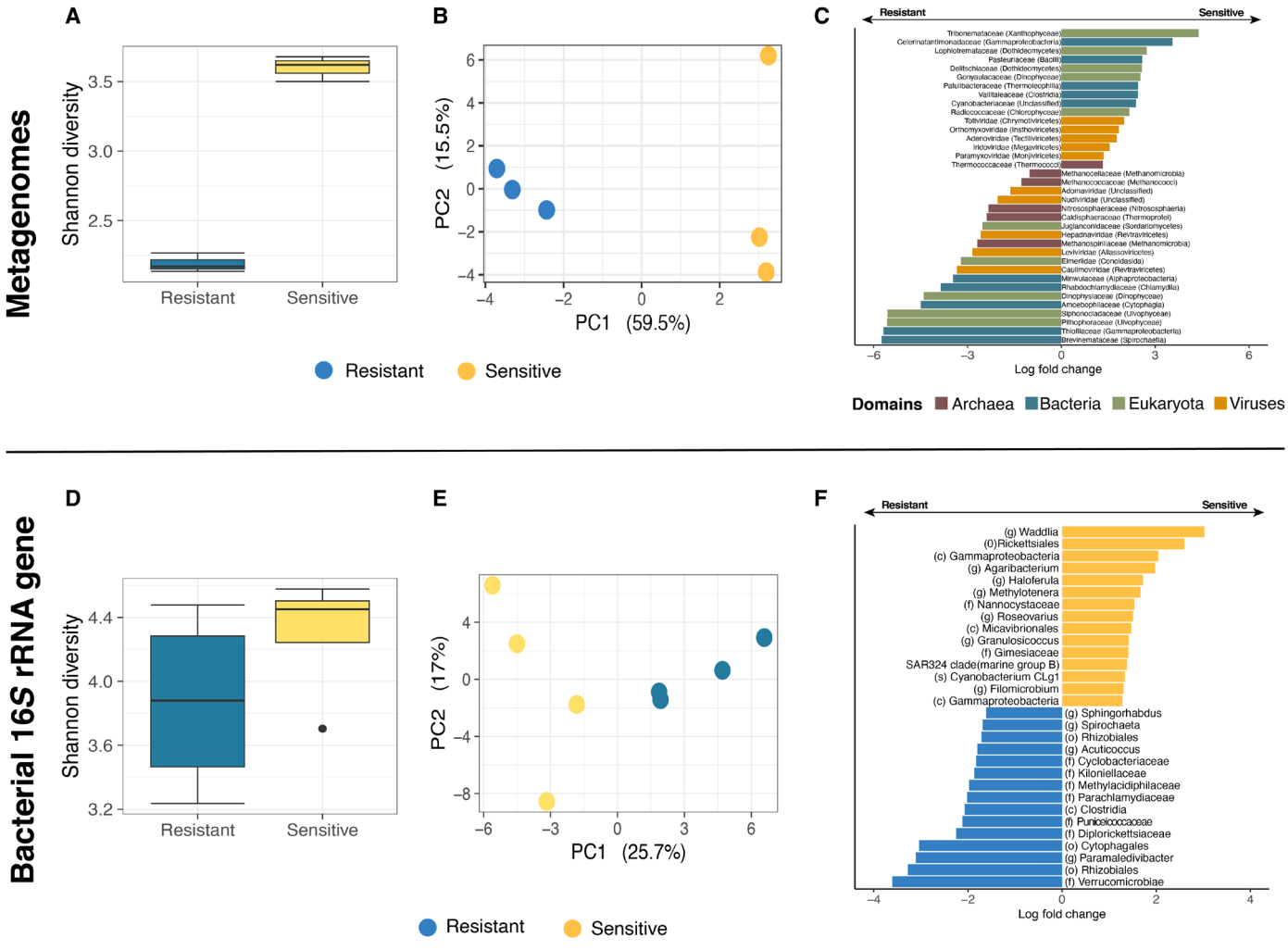

Fig. 3. Microbial assemblages associated with TBR and TBS coral phenotypes. Alpha diversity (Shannon diversity) (**A**) and beta diversity (**B**) of metagenomic families (or the highest assigned taxonomic level) of different coral phenotypes of the overall community in T0. (**C**) Bar plots with the metagenomic differentially abundant (DA) families in TBR and TBS corals, in which LFCs with negative values are referred to as resistant phenotype, whereas positive values are referred to as sensitive phenotype. Alpha diversity (**D**) and beta diversity (**E**) of bacterial genera of the 16*S* rRNA gene sequencing. (**F**) Bar plots with DA genera (or the lowest identified taxonomic level) in resistant (negative LFC values, blue) and sensitive (positive LFC values, yellow) corals. The taxonomic classifications presented in the DA analysis reflect varying taxonomic levels (genus, family, and class), as many relevant bacterial groups could not be consistently classified at a more specific level.

those involved in carbohydrate (58 DAs), lipid (32 DAs), and energy metabolism (36 DAs). These microeukaryotic metabolic KOs were mainly part of biosynthesis pathways, such as the biosynthesis of terpenoids and polyketides (e.g., Oleandomycin biosynthesis and Maduropeptin beta-hydroxy acid moiety biosynthesis; see table S9 for ANCOM-BC values), biosynthesis of sugars and glycerophospholipids [e.g., glycosylphosphatidylinositol (GPI)-anchor, glycogen phosphorylase, *N*-acetylgalactosaminyltransferase 3], photosynthesis (*psbA*, *psbD*, and *petB*), and oxidative phosphorylation [e.g., V/A-type adenosine triphosphatase (ATPase), F-type ATPase] in TBR corals (Fig. 4E].

In contrast, TBS corals exhibit a predominance of bacterial KOs involved in carbohydrate metabolism (41 DAs), protein metabolism (37 DAs), amino acid metabolism (29 DAs), and metabolism of cofactors and vitamins (20 DAs). For instance, bacterial KOs such as nitrilase (nitrogen metabolism), Syringomycin synthetase protein SyrB1 (amino acids metabolism), ketoreductase RED1 (metabolism of terpenoids and polyketides), and lysophospholipid acyltransferase (lipid metabolism) were the most differentially abundant bacterial KOs in TBS corals (table S9 and Fig. 4D).

Changes in microbiome assemblages in response to heat stress

Microbial composition of different phenotypes under thermal stress

We also investigated the microbiome's response to heat stress by comparing the microbial community between sampling times within each coral phenotype separately using ITS2 sequencing, metagenomic shotgun sequencing, and 16*S* rRNA gene sequencing. The Symbiodiniaceae composition of both TBR and TBS corals remained stable and did not change due to the heat stress (from T0 to T1) (PERMANOVA, $P = 0.25$, $R^2 = 0.02$; Fig. 2B and table S2).

In TBR corals, the overall metagenomic diversity at the family level decreased from T0 to T1 (Shannon Index, ANOVA, $P = 0.003$;

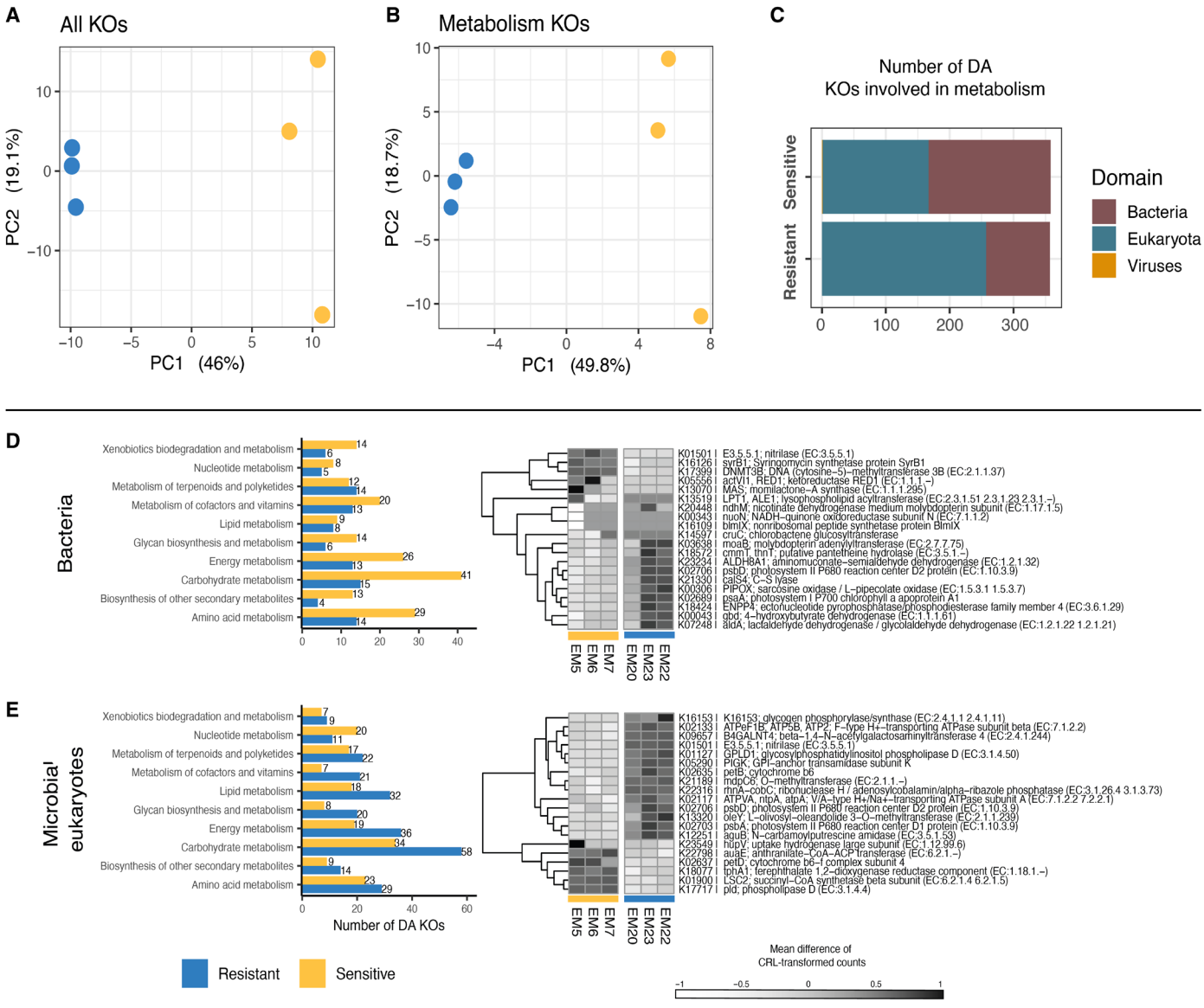

Fig. 4. Differences in the metabolic profiles of TBR and TBS corals maintained under the same environmental conditions (T0). (**A**) Ordination plots of all metagenomic KOs and (**B**) KOs related to metabolism in TBR and TBS corals. (**C**) Number of DA metabolic KOs distributed across domains in the coral phenotypes. Heatmap of DA metabolic KOs (right) and their KO L3 categories to which the KOs were assigned to (left) found in (**D**) bacteria and (**E**) microbial eukaryotes in TBR and TBS corals.

table S3 and fig. S3). Changes in the 16*S* rRNA bacterial community were observed only for beta diversity (PERMANOVA, $P = 0.007$, $R^2 = 0.1$; table S6), not only during the stress period (T0 versus T1, PERMANOVA, $P = 0.042$, $R^2 = 0.02$; table S6) but also after the recovery period (T1 versus T2, PERMANOVA, $P = 0.042$, $R^2 = 0.02$; figs. S3 and S4 and table S6).

Analysis of metagenomic data of TBS corals did not indicate significant differences in alpha diversity (Shannon index, ANOVA, $P = 042$; table S3) or taxonomic composition between T0 and T1 (PERMANOVA, $P = 0.7$, $R^2 = 0.15$; table S3). In contrast, the analysis of the bacterial communities through 16*S* rRNA gene amplicon sequencing revealed significant shifts in the structure of the bacterial community of TBS corals at the peak of temperature (T0 versus T1, PERMANOVA, $P = 0.042$, $R^2 = 0.17$; figs. S3 and S4 and table S6). No significant changes were detected after the recovery period (T1 versus T2, PERMANOVA, $P = 0.097$, $R^2 = 0.18$; figs. S3 and S4 and table S6).

Functional profiles do not change over time or under stress

Changes in the microbial community (i.e., bacterial community, as shown in the section above) throughout the experiment and during heat stress did not result in any apparent significant changes in overall functions (PERMANOVA, $P = 0.255$, $R^2 = 0.07$; table S8) or in any differentially abundant KO between the sampling times evaluated (T0 versus T1) within phenotypes.

DISCUSSION

Distinct bleaching responses

In this study, two different phenotypes of the coral *M. hispida* demonstrated different bleaching responses during a long-term heat

stress experiment. Despite the lack of consensus in the literature regarding the use of the term thermal resistance for corals or other marine organisms, we followed the definition provided by Matsuda and colleagues (*10*), which defines bleaching resistant corals as those that maintain their pigmentation during a bleaching event. We used the Coral Health Chart as a color reference to assess bleaching, defining bleaching as the decrease of two or more color units (*38*). This approach enabled us to categorize the different phenotypes of *M. hispida* as either thermally-resistant (TBR) or thermally-sensitive (TBS) corals. Ten days of exposure to an acute heat stress caused bleaching and mortality in TBS corals. Significant decreases in the TBS corals' F_v/F_m rates indicate temperature-related damage to the photosystem II (PSII) electron transport of the Symbiodiniaceae, which is consistent with the loss/expulsion of Symbiodiniaceae and visual signs of bleaching (*39*). Although TBR corals exhibited no visible signs of bleaching, even when exposed to higher temperatures than TBS corals, some fluctuations in the F_v/F_m rates during heat stress were observed. Despite this drop in the F_v/F_m rates in T1, TBR corals restored their F_v/F_m rates during the recovery period (T2).

Inherent differences in the host-Symbiodiniaceae-microbiome assemblages and their functional contributions

Beyond examples such as physiological acclimatization (*8*), host adaptation (*8*, *40*), and the assisted migration of heat-tolerant alleles (*9*, *41*), the association of corals with specific groups of Symbiodiniaceae (*10*) or other microbial assemblages (*19*) represents additional mechanisms that may contribute to thermal bleaching resistance. TBR and TBS corals inherently harbor significant taxonomic differences even under non-stress ambient conditions (i.e., T0). First, TBR corals were dominated by the *Symbiodinium* A4 type, followed by a small portion of *Cladocopium* C21-C3vv-C3-C3vw-C50br, whereas TBS corals mainly hosted *Cladocopium* C3-C3vv-C3ww-C3-C50br-C3vu followed by *Symbiodinium* A4/A1-A4br-A4bq-A1mi-A1b. Both *Symbiodinium* A4 and *Cladocopium* C3 are widespread and generalist ITS2 types (*42*) that are commonly found in corals of the genus *Mussismilia* (*43*). Previous studies have demonstrated that *Cladocopium* C3 is more frequently associated with mild temperature and high light conditions, whereas *Symbiodinium* A4 is more commonly present in shallow waters and under higher irradiance (*44*). In addition, the TBR-dominant *Symbiodinium* A4 has been reported to facilitate positive growth rates at high temperature in experiments in hospite (i.e., in association with *Porites divaricatea*) (*45*). Despite differences in the dominant Symbiodiniaceae types between TBR and TBS, both phenotypes maintained a stable algal community composition, even when heat stress was applied. Although the inherent differences between TBR and TBS corals may stem from specific responses to past temperature stress and/or environmental factors from their original site, the long-term rearing of these corals under the same aquarium conditions suggests adaptation to the current environment (*46*). This enables us to explore alternative mechanisms contributing to coral bleaching resistance, providing insights beyond site-specific factors.

TBR corals harbored a higher relative abundance of eukaryotes (predominantly Symbiodiniaceae) compared to TBS corals. The higher relative abundance of Symbiodiniaceae and other dinoflagellates, such as Dinophysiaceae, in TBR corals is also reflected in the enrichment of photosynthetic genes such as *psbA*, *psbD*, and *petB*, which encode the D1, D2, and cytochrome b6 proteins—core components of the photosynthetic apparatus in algae and other photosynthetic organisms (*47*, *48*). This observation aligns with the dominance of Symbiodinium A4 ITS2 type in TBR corals, which has been previously reported to enhance growth rates at high temperatures (*45*).

Furthermore, disparities in microbial structure and composition mirrored and seem to influence the distinct functional profiles observed in each coral phenotype. For example, microeukaryotes contributed significantly to genes associated with catabolic pathways in TBR corals, while bacteria were the main contributors to metabolic genes associated with TBS corals. The biosynthesis of GPI-anchor proteins, specifically GPI phospholipase D and GPI-anchor transamidase subunit K, was significantly enriched in TBR corals. These proteins play crucial roles in cell wall assembly, hardening, and softening (*49*, *50*). In symbiotic dinoflagellates, the cell wall tends to be thinner to facilitate nutrient exchange and communication (*51*, *52*), potentially enhancing the metabolic exchange between Symbiodiniaceae and other members of the microbiome. This closer interaction could, in turn, foster specific microbial assemblages that support the resistance of TBR corals. Moreover, GPI-anchor proteins have been proposed as alternative phosphate sources under mildly acidic pH or phosphate-limited conditions (*53*), although the exact role of these proteins in cnidarian-dinoflagellate symbiosis under thermal stress requires further investigation. In addition, TBR corals showed enrichment in oleandomycin and maduropeptin biosynthesis. While both compounds exhibit substantial antibiotic properties (*54*), maduropeptin also demonstrates potent antitumor activity by targeting rapidly dividing cells (*55*). These bioactive molecules could, for example, be involved in controlling pathogens and/or fast-growing organisms within the microbial community of TBR corals, potentially contributing to their overall resistance to thermal stress (*56*).

The balance between eukaryotic and bacterial players may contribute to TBR corals being proportionally enriched in metabolic pathways related to the metabolism of carbohydrates and proteins, which could shape their microbial associations. Similar to free-living phytoplankton and other microbial eukaryotes, Symbiodiniaceae have been hypothesized to exude metabolites creating an enriched zone around themselves (*57*, *58*), which attracts and supports the growth of other microorganisms (*59*, *60*). Known as the "phycosphere," this physical interface might selectively promote associations with other microbial eukaryotes, bacteria, archaea, and viruses (*61*, *62*). Our results point to a potential differential phycosphere effect in TBR and TBS corals (*62*), which could selectively enrich particular bacterial groups associated with in hospite Symbiodiniaceae (*31*). Consequently, this could influence the corals' phenotypic responses and levels of thermal resilience.

In addition, all microbial groups, including microbial eukaryotes, viruses, archaea, and bacteria, seem to differentially associate with each phenotype. For example, compared to TBS, TBR corals present an enrichment of the dinoflagellate Dinophysiaceae, which belongs to the same class as their Symbiodinaceae counterparts (Dinophyceae and Alveolata) (*63*). The annotation of several genes of Dinophyceae, including percentage where available, suggests their affiliation within the Symbiodiniaceae family. However, due to the resolution limitations inherent to gene-based taxonomy, particularly in metagenomic approaches, these sequences could not be classified at a more specific taxonomic level within the family. This is a common challenge in metagenomic studies, where the available

genetic markers often lack the precision needed for higher-resolution classifications. Nevertheless, the enrichment of either Dinophyceae or Symbiodiniaceae may potentially contribute to their overall fitness and/or to attracting other microbes due to their photosynthetic capacity.

Viruses such as Leviviridae and Hepadnaviridae were also inherently enriched in TBR corals. Bacteriophages play a crucial role in shaping bacterial populations within the coral microbiome by selectively targeting specific bacterial species. For instance, Leviviridae, previously detected in soil ecosystems, have been shown to regulate populations of Gammaproteobacteria and Alphaproteobacteria (*64*–*66*), which could similarly contribute to microbial regulation in corals. While Hepadnaviridae are primarily associated with vertebrates, they have been occasionally identified in corals (*67*). However, their low abundance in metatranscriptomic data suggests that these viruses are not highly active, possibly leading to an underestimation of their influence (*68*).

Archaea are also known to play crucial roles in various extreme ecosystems, including contaminated and methanogenic soil (*69*) and hydrothermal vents (*70*). Although not commonly reported in corals, Caldisphaeraceae, Methanospirillaceae, and Nitrososphaeraceae are thermophilic archaea typically found in harsh environments and were also inherently enriched in TBR corals. In TBR corals, these archaea may contribute to nutrient cycling and ammonia oxidation (*71*), as they do in other ecosystems, potentially supporting the resilience of these corals under thermal stress conditions.

While metagenomic taxonomic profiling provides a broader overview of the microbiome, 16*S* rRNA gene sequencing offers greater taxonomic resolution for identifying specific bacterial groups. Although groups such as Rhizobiales, Clostridia, *Paramaledivibacter*, and Cytophagales were not detected as differentially abundant in the metagenomic analysis comparing coral phenotypes, ASVs from these groups were enriched in TBR corals. Both Clostridia and Rhizobiales have been associated with coral tissue loss and lesion progression in previous studies (*72*). However, discerning between detrimental and beneficial organisms within the complex coral holobionts is particularly challenging (*73*–*75*). For example, Rhizobiales are known to form symbiotic relationships with plants, contributing to nitrogen fixation, methane oxidation, and microsymbiosis (*76*, *77*). Similarly, Young *et al.* (*78*) reported a strong correlation between the expression of healing genes and diseased corals, suggesting that microbial responses to stress may not directly indicate disease progression but may instead reflect a protective or regulatory role performed by the microbiome.

Spirochaeta and *Sphingorhabdus* were also inherently enriched in TBR corals. Members of the *Spirochaetaceae* family are nonpathogenic, free-living anaerobes known for their ability to fix nitrogen (*79*) and degrade organic carbon (*80*), and have been previously identified in *Acropora palmata* (*81*) and various color morphs of *Corallium rubrum* (*82*). Cultures of the thermotolerant *Symbiodinium pilosum* were found to be dominated by *Sphingorhabdus* [Díaz-Almeyda *et al.* (*83*)]. *S. pilosum* exhibits high thermal tolerance, showing no decline in growth rate or photochemical efficiency even at 32°C (*83*). Although *Sphingorhabdus* has been detected and isolated from gorgonian corals (*84*, *85*), its broader role remains underexplored. Further research could uncover its role in supporting *S. pilosum* and the holobiont's thermotolerance, offering insights into coral resilience mechanisms, suggesting their potential as markers for tracking thermally resistant corals or as candidates for future studies on beneficial microorganisms. The enrichment of taxa previously associated with diseased corals together with bacteria with known beneficial traits in TBR suggests a dynamic biological regulation by the host and/or other biological forces within the holobiont.

In TBS corals, specific bacterial taxa such as Celerinatantimonadaceae, Pasteuriaceae, members of the Rhodobacteraceae family (uncategorized ASVs and *Roseovarius*), Rickettsiales, *Waddlia*, and *Agaribacterium* were inherently enriched. While some of these taxa, such as Celerinatantimonadaceae, Pasteuriaceae, and *Agaribacterium*, are not well documented in corals or other marine organisms, others are commonly associated with disease. Members belonging to the Rhodobacteraceae family, for example, are commonly found in development and progression of coral disease and sewage (*86*–*88*). Rickettsiales are Gram-negative bacteria known to cause diseases in invertebrates (*89*, *90*). *Waddlia*, and other species classified within the Chlamydia-like group have demonstrated to be strong cytopathic-diseased vectors in fish cell lines (*91*). In addition, TBS corals showed an enrichment of bacterial metabolic genes, similar to previous findings where diseased coral tissues were enriched with bacterial sequences, compared to healthy tissues (*92*).

Metabolic redundancy in corals under stress

Although some shifts in the microbiome structure are observed throughout time as a response to the applied heat stress, no overall changes were detected in the functional profile of either TBR or TBS corals. This may suggest some level of metabolic redundancy, in which taxonomic changes are observed, but these shifts are, somehow, regulated in a manner that functions remain the same (*93*, *94*). This is one strategy some holobionts may use to maintain its homeostasis. On the basis of our observation, the "winner holobiont" seems to depend on the baseline and inherent holobiont assemblage before any stress is applied, indicating that these specific assemblages underscore determined functions that may support coral holobionts during heat stress.

In our study, we found specific Symbiodiniaceae-microbiome assemblages inherently associated with distinct TBR and TBS phenotypes of *M. hispida*. In addition, the proportion of microbial eukaryotes and bacteria harbored by either TBR or TBS corals seems to directly influence the metabolic profile of these phenotypes, especially their metabolism of proteins, carbohydrates, and energy. More specifically, TBR corals exhibited an inherent enrichment of microbial eukaryotes, especially Symbiodiniaceae, which was mirrored by the enrichment of key functions such as photosynthesis, membrane anchoring, and the production of antibiotic and antitumor proteins. The biosynthesis of GPI-anchor proteins, which are essential for processes like cell wall assembly and regulation of its hardening and softening, was also notably enriched in TBR corals and may contribute to the exchange of metabolites between Symbiodiniaceae and other members of the holobiont. Conversely, TBS corals showed a predominance of bacterial metabolic genes, particularly those involved in nitrogen cycling, amino acid synthesis, and lipid metabolism. Although the observed differences between TBR and TBS can be driven by several factors, such as past environmental conditions, we hypothesize that these distinct and consistent multidomain microbiome assemblages comprise distinct holobiont phenotypes (Fig. 5). It is important to highlight that the differences between TBR and TBS corals reported in this study are inherent, e.g., observed at the beginning of the experiment when all corals were under the same environmental conditions. This baseline distinction suggests that the

observed microbial differences are associated to the different phenotypes and not merely (or only) a result of thermal stress and other environmental conditions, providing a profound insight into the correlation between corals, their thermal phenotypes, and their associated microbiomes. These insights lay the ground for further investigations that can support rehabilitation approaches, such as the selection of coral probiotics aimed at mitigating coral mortality in the future climate scenario.

METHODS

Ethics approval and consent to participate

Permission for sampling was obtained from the Brazilian authorities System of Authorization and Information on Biodiversity under license number 54429-1. The microbial survey permits were obtained from the National Council for Scientific and Technological Development and the National System for the Management of Genetic Heritage and Associated Traditional Knowledge under license number A620FE5.

Coral colonies

The *M. hispida* colonies used in this study were part of a collection from the AquaRio, Rio de Janeiro, Brazil. These colonies were collected in the Abrolhos region, Bahia, Brazil about 6 months before the main experiments and kept in tanks at 26°C. Daily sea surface temperature data from the Abrolhos reef station are available in table S10, of which 26°C corresponds to the annual mean in this area, as also reported in (*95*). A pilot test was conducted before the main experiment to define thermal stress resistance of these *M. hispida* colonies. The pilot experiment is detailed in Supplementary Materials and Methods (data were only observational). Briefly, twenty individual *M. hispida* colonies were fragmented using a diamond band saw (Gryphon Corp., Los Angeles, CA, USA), generating fragments with at least three polyps (~7 cm). The fragments were labeled

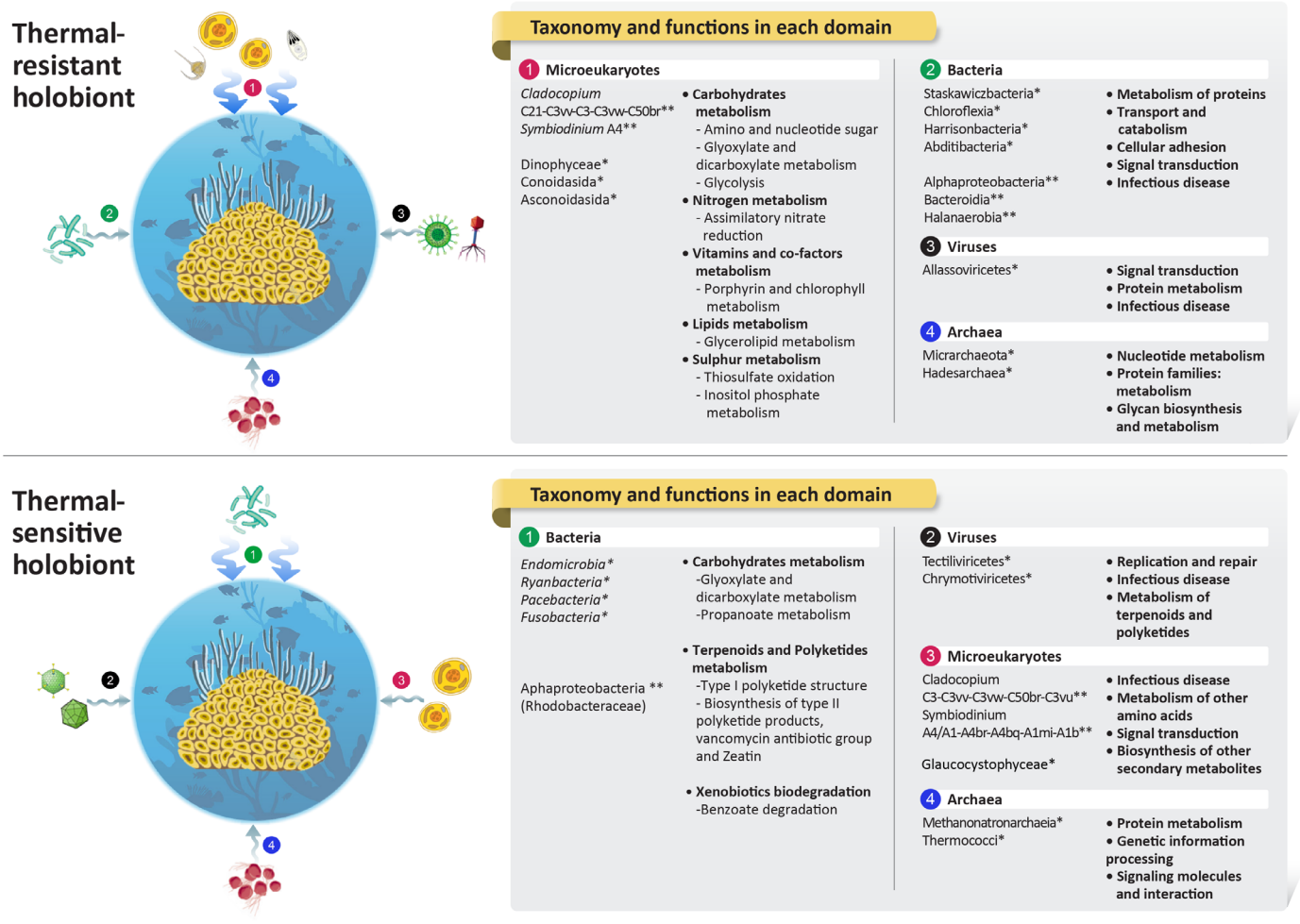

Fig. 5. Microbial assemblages and the metabolic profiles associated with TBR and TBS coral phenotypes. Taxonomy and metabolic functions associated with TBR and TBS phenotypes. Taxa recovered from metagenomes are reported at the family level, whereas taxa recovered from 16*S rRNA* gene sequencing are reported at the lowest level found. The metabolic functions enriched by the different domains are not necessarily connected to the taxa enriched and reported in the figure. The thick blue arrows indicate the microbial groups contributing a considerably higher portion of genes involved in the holobiont's metabolism. The morphology of microorganisms in this figure is merely illustrative and represents the general morphology of one representative organism from the mentioned family. *Recovered from metagenomes. **Recovered from amplicon sequencing (16*S* rRNA gene for bacteria and ITS2 for Symbiodiniaceae).

as per their corresponding colony of origin and some of them were used to run the pilot test (*96*). Coral individuals categorized as TBS bleached at 30.5°C, whereas no visual signs of bleaching were observed in the TBR corals at the same temperature. The results of the pilot tests guided the experimental design described in the Thermal stress experiment section. Following the pilot test, additional fragments (ramets) from the corresponding TBS or TBR colonies were used in the thermal stress experiment.

Experimental mesocosms setup

The mesocosm used for the experiments consisted of two water baths, one for each temperature regime/phenotype. Each water bath had four individual aquariums (15 cm by 11 cm by 12 cm) connected to their individual 26-liter sumps. A total of 10 liters of seawater was in constant circulation between the sumps and the aquariums (1 liter in the aquarium and 9 liters in the sump) by a water pump (Mini A, Sarlo Better, São Caetano do Sul, Brazil), at a 250–ml min^{-1} flow rate, providing a 15-fold recirculation of the aquarium volume per hour. Every two days, 10% of the water from each individual sump was replaced, and the salinity was measured and adjusted with ultrapure water when necessary. The water used in the experiment consisted of seawater collected monthly by AquaRio in the Cagarras Islands surrounding areas (23° 1 ′57.23″S; 43° 9′ 17.18″W; Rio de Janeiro, RJ, Brazil). Upon arrival in Aquario's facilities, the portion of water designated for the experiment was transferred to 1000-liter containers and used to supply the experimental sumps/aquariums when water changes were necessary. This water was also kept in constant circulation by water pumps (Better 2000, Sarlo Better) for the entire period of the experiment. Each individual aquarium represented one biological replicate and there were four replicates per treatment (Fig. 1A). Physical-chemical water parameters, as pH and dissolved oxygen, were measured during the sampling times using a multiparameter probe (model HI 9828, Hanna Instruments, Barueri, São Paulo) and are provided in table S11. Each aquarium received an individual air-bubbling system that was provided by an air pump (HG-370, Sun Sun) connected to silicone air hoses and flow controllers. The water baths' temperature was controlled by temperature controls MT-518ri (Canoas, Brazil), and the water was circulated by two aquarium pumps (SB 1000A, Sarlo Better). The mesocosm was artificially illuminated with an irradiance of 350 µmol photons m^{-2} s^{-1} and followed a natural day:night 12:12-hour cycle. The mesocosm setup can be seen in fig. S5.

Thermal stress experiments

Each experimental aquarium was randomly assigned to receive three fragments (rametes) from one single colony of TBR or TBS (i.e., one aquarium per genotype). A total of four aquariums per phenotype were placed in their respective water baths (Fig. 1A; see fig. S5 for detailed mesocosm diagram). For consistency, one fragment from each tank was used to measure the F_v/F_m throughout the experiment (i.e., the fragment collected at the last sampling time, T2). After 10 days of acclimatization in the mesocosm at 26°C, one fragment of each tank was randomly collected (T0). Then, the temperature was gradually increased by 0.5°C per day to reach "pre-peak temperature" (30.5°C for TBR and 29.5°C for TBS corals) (*15*, *16*). Coral fragments were maintained at pre-peak temperature for 10 days. Subsequently, the temperature was again increased (0.5°C/day), up to 32°C for resistant fragments and 30.5°C for the sensitive ones, and kept at this temperature peak for 4 days. After this period, a second fragment per tank was collected (T1) followed by the gradual decrease of temperature to 26°C (0.5°C per day). After 15 days of recovery at 26°C, the last fragment from each tank was collected (T2). The temperature regime used for each TBR and TBS can be seen in Fig. 1A. The sampling procedure always occurred before temperatures were changed and at the same time of day (mornings). The experiments lasted a total of 51 and 45 days for TBR and TBS, respectively, representing long-term experiments as defined by Grottoli and colleagues (*97*). The sampled fragments were photographed for bleaching scoring and snap-frozen in liquid nitrogen and then transferred to a −80°C ultra-freezer until further analysis.

Coral health assessment

Coral health was assessed via visual bleaching scoring and measurement of the endosymbiotic algae's photosynthetic efficiency (F_v/F_m). Visual bleaching was assessed from pictures taken of coral fragments using a Canon T3i digital camera and the Coral Health Chart (University of Queensland) as a color reference (*38*). As each aquarium contained fragments from the same colony, the sampled fragment was used as a representative of the bleaching status of the biological replicate. Corals that decreased by two or more units of color between T0 and the comparing sampling times were considered bleached (*98*).

The endosymbiotic algae's photosynthetic efficiency (F_v/F_m) was measured throughout the experiment using a diving pulse amplitude–modulated (PAM) fluorometer (Walz GmbH, Effeltrich, Germany) fitted with a blue-emitting diode LED. The values corresponding to the sampling times were taken the night before sampling. To avoid nonphotochemical processes of the PSII excitation energy's dissipation, measurements were taken after sunset, with at least 30 min of dark adaptation. The maximum quantum yield of PSII photochemistry was determined as F_v/F_m. The diving PAM-fluorometer was configured as follows: measuring light intensity, 5; saturation pulse intensity, 8; saturation pulse width, 0.8; gain, 2; and damping, 2. For consistency, one fragment from each tank was used to measure the F_v/F_m throughout the experiment (i.e., the fragment collected at the last sampling time, T2). Changes in the F_v/F_m through time within phenotypes were analyzed by fitting a linear mixed effect model using the "lmer" function from lme4 package in R studio (version 4.2.3) (*99*). Colonies (biological replicates, $n = 4$) were treated as a random effect on the intercept to account for the nonindependence of replicates with time. Fixed and random effects were tested using likelihood-ratio t tests ($\alpha = 0.05$). Pairwise contrasts were estimated by using the "emmeans" package using pairs of sampling times (T0 × T1; T0 × T2; T1 × T2) for each phenotype group (TBR and TBS) individually. The package "ggplot" was used to generate the graphs. The script is available in the GitHub link found at the data and materials availability section.

DNA extraction and ITS2, 16*S*, and metagenomics sequencing

Sampled coral fragments were macerated with sterile mortar and pestle using liquid nitrogen. The total DNA was extracted from 0.5 g of the macerated sections (mucus/tissue/skeleton) using the Power-Biofilm DNA Isolation kit (MoBio Laboratories Inc.) as per the manufacturer's procedures. In addition to our samples, one extraction was made with no biological material input to check for kit contamination, which was included in all further amplicon sequencing steps as a negative control. The DNA concentration was determined

using a Qubit 2.0 Fluorometer High Sensitivity DNA Kit (Invitrogen, USA). The samples used for each of the analyses are described in table S12.

For the characterization of the Symbiodiniaceae community, we used amplicon sequencing of the ITS2 region of the rRNA gene only from T0 and T1 samples ($n = 13$: three of four replicates from each respective sampling point and one negative DNA extraction control). Extracted DNA aliquots were dried into GenTegra-DNA 0.5-ml screw cap tubes (https://gentegra.com/gentegra-dna-2/, Pleasanton, California, USA) and shipped to the University of Konstanz. There, DNA samples were reconstituted in 30 μl of molecular-grade water (GenTegra-DNA) in 0.5-ml screw cap microtubes according to the manufacturer's protocol. Concentration of reconstituted samples was determined using the Qubit 2.0 Fluorometer High Sensitivity DNA Kit (Invitrogen, USA) to determine the amount of DNA used in the subsequent steps. Amplification of the ITS2 region was completed using the Qiagen Multiplex polymerase chain reaction (PCR) kit, with 1 to 5 ng of DNA from each coral sample using the primers SYM_VAR_5.8S2 [5′-GAATTGCAGAACTCCGTGAACC-3′] and SYM_VAR_REV [5′-CGGGTTCWCTTGTYTGACTTCATGC-3′] (*100*) with unique 8-mer barcodes at the respective 5′ ends at a final primer concentration of 0.5 μM in a reaction volume of 10 μl. Thermal cycler conditions for ITS2 PCR amplification were as follows: initial denaturation at 95°C for 15 min, 35 cycles at 95°C for 30 s, 56°C for 90 s, and 72°C for 30 s, followed by a final extension step at 72°C for 10 min. To confirm successful amplification, 1 μl of each PCR product was run on a 1% agarose gel. The samples were cleaned using ExoProStar 1-step (GE Healthcare) and normalized using the SequalPrep Normalization Plate Kit (Thermo Fisher Scientific). The samples were then pooled into a 1.5-ml Eppendorf tube (17 μl per sample) and concentrated using a benchtop Speedvac (Concentrator plus, Eppendorf). Quantification was completed using Qubit (Qubit dsDNA High Sensitivity Assay Kit, Invitrogen), and the samples were paired-end sequenced [2 base pair (bp) by 250 bp] on the NovaSeq 6000 platform at the Novogene Sequencing Centre (Cambridge, England).

Furthermore, shotgun sequencing was used to sequence metagenomes from both TBS and TBR samples at the beginning of the experiment (T0) and after the peak of temperature (T1) ($n = 12$). Extracted DNA aliquots were shipped frozen on dry ice to the Argonne National Laboratory (http://ngs.igsb.anl.gov, Lemont, IL, USA). Upon arrival, DNA concentration was measured by Qubit assay (Qubit dsDNA High Sensitivity Assay Kit, Invitrogen) and 500 ng of DNA was sheared using the Covaris S-series system to obtain 200- to 500-bp fragments. Takera's PrepX kit was used for sequence library preparation. Since the libraries did not reach a 2 nM concentration (Qubit DNA HS Assay kit), a PCR was performed using the primers [5′ - GATCGGAAGAGCACACGTCTGAACTCCAGTCACXXXXXXATCTCGTATGCCGTCTTCTGCTTG-3] and [5′-AATGATACGGCGACCACCGAGATCTACACXXXXXXACACTCTTTCCCTACACGACGCTCTTCCGATCT-3′], in which the 6-X sequence is the unique sample's indexes, and then following the conditions: 2 min at 98°C, 10 to 15 cycles of 30 s at 98°C, 30 s at 65°C, 60 s at 72°C, and 4 min at 72°C. Library size and quality were then again determined by a Qubit assay (DNA HS Assay kit) and with the Agilent 2100 Bioanalyzer, respectively. The libraries were sequenced at 15 pM on a pair-ended 2 bp–by–150 bp sequencing run on Illumina's HiSeq 2000 (Illumina, San Diego, CA, USA) as per the manufacturer's guidelines.

For the characterization of prokaryotic communities, the primers 515F and 806R (*101*) were used to amplify the 16*S* rRNA gene V4 variable region. Samples from T0, T1, and T2 ($n = 24$: 4 samples from each of TBR0, TBR1, and TBR2 for a total of 12 samples; 11 samples in total from 4 samples TBS0, 4 samples TBS1, and 3 samples TBS1; and 1 negative DNA extraction control—Note that one replicate of TBS coral died before T2) were shipped frozen on dry ice to Argonne National Laboratory (http://ngs.igsb.anl.gov, Lemont, IL, USA) to be sequenced. PCRs, using 1 μl of input DNA, were performed in triplicates using the QIAGEN Multiplex PCR kit, with a final primer concentration of 0.2 μM in a final reaction volume of 25 μl. Thermal cycler conditions were as follows: initial denaturation at 94°C for 3 min, 35 cycles at 94°C for 45 s, 50°C for 60 s, and 72°C for 90 s, followed by a final extension at 72°C for 10 min. The corresponding triplicates from each sample were then pooled, and 5 μl of each PCR product was run on a 1% agarose gel to confirm successful amplification. The samples were cleaned using the MoBio UltraClean PCR Clean-Up Kit and indexed using the Nextera XT Index Kit v2 (with dual indices and Illumina sequencing adaptors added). The successful addition of indexes was confirmed by comparing the initial PCR product's length with the corresponding indexed sample on a 1% agarose gel. The samples were cleaned and normalized using the SequalPrep Normalization Plate Kit (Invitrogen, Carlsbad, CA, USA). The library quality was assessed using the Agilent High Sensitivity DNA Kit in an Agilent 2100 Bioanalyzer (Agilent Technologies, Santa Clara, CA, USA) and quantified using the Quant-iT PicoGreen dsDNA Assay Kit (Thermo Fisher Scientific/Invitrogen) as per the manufacturer's instructions. Libraries were paired-end (2 bp by 250 bp) sequenced at 5 pM with 20% phiX on the Illumina MiSeq Illumina platform at the Argonne National Laboratory (http://ngs.igsb.anl.gov, Lemont, IL, USA). All sequences generated in this study are available in the National Center for Biotechnology Information (NCBI) database under the BioProject PRJNA607335.

ITS2 Symbiodiniaceae and 16*S* rRNA gene prokaryotic analysis

The SymPortal framework (https://symportal.org/) was used to analyze the ITS2 sequencing data (*102*). Briefly, demultiplexed paired-ended ITS2 sequencing files were submitted to SymPortal, which includes a pipeline for quality control (QC) using mothur 1.43.0 (*103*), the blast+ suite of executables (*104*), and minimum entropy decomposition (*105*). After QC steps, ITS2 type profiles were inferred and characterized by specific sets of defining intragenomic ITS sequence variants (which represent putative Symbiodiniaceae lineages or genotypes). SymPortal-output were used to plot ITS2 sequence counts and ITS type profile abundance tables as well as the Bray-Curtis–based matrices for between-samples and between-ITS2 types profile comparisons. Samples from the T0 and T1 sampling times from both TBR and TBS corals and a negative control were used for this analysis ($n = 13$).

Furthermore, demultiplexed and adaptor-free sequences were used to infer 16*S* rRNA gene ASVs using DADA2 v1.21.0 (*106*). Forward and reverse reads were truncated at the 3′ ends of the 240 and 200 bp, respectively. Reads with expected errors >2 or with the presence of ambiguous bases were discarded. ASVs inferred from individual read pairs were merged and checked for chimeras and subsequently annotated using the SILVA database, version 138 (*107*). Sequence reads statistics and ASV raw counts

are shown in table S13. A total of 3260 ASVs were inferred from the 24 samples (12 samples from TBR0, TBR1, and TBR2; 11 samples from TS0, TS1, and TS1; and 1 negative control). Putative ASV contaminants were identified as those with sample-to-negative control ratios greater than 10%. Contamination ratios were calculated as the mean relative abundance across biological samples divided by the mean relative abundance across negative controls (resulting from a reaction with no DNA added), divided by 100. After removing putative contaminants and ASVs classified as mitochondria and chloroplasts, 2660 ASVs were retained for downstream analysis. ASVs identified as putative contaminants, as well as mitochondria and chloroplasts can be found in table S14. Phyloseq v1.4 (*108*) was used to calculate beta diversity from Euclidean distances of centered-log ratio (clr)–transformed ASV counts, which were then represented on a constrained principal components analyses (PCA) calculated with the redundancy analysis function. Statistical differences between bacterial community composition among samples were tested using PERMANOVA, and variance homogeneity across groups (phenotype × time) was tested using PERMADISP with the adonis and betadisper functions, respectively, implemented in the R package Vegan v2.5 (*109*). Alpha diversity was calculated using the Shannon diversity index from rarefied abundances to a sample count of 6729 (corresponding to the minimum library size) using the Rarefy function from the GUniFrac v1.7 package (*110*). Linear models were fit to test for differences in alpha diversity between phenotypes and time points with the formula Shannon~phenotype*time using the lm function of the stats v4.2 package. Eta-squared values were calculated for linear models to indicate the partial association of each term in the multivariate linear model using the EtaSq function of the DescTools R package. Residuals were tested for normality using the Shapiro-Wilk normality test (W = 0.93, *P* value = 0.14). Pairwise comparisons were conducted using the emmeans package v1.8.2 (*111*). Differential abundance analysis of bacterial ASVs was completed using ANCOM-BC v1.0.5 through an ANCOM-BC (*112*) to identify differentially abundant taxa between phenotypes and time points. Differentially abundant ASVs between coral phenotypes and time points were identified using ANCOM-BC v.1.0.2 with false discovery rate (FDR)–adjusted *P* values <0.05.

Taxonomic and functional analysis of the microbiome through metagenomics

Adapters and bases with Q < 15 were trimmed, and reads shorter than 75 nt were removed using Trimmomatic v0.38 (*113*). Metagenomics sequencing size and coverage depth can be found in table S15. Metagenome assemblies using MEGAHIT v1.2.9 (*114*), SPAdes v3.13.0 (*115*), and IDBA v1.1.3-1 (*116*) were evaluated using QUAST v5.0.2 (*117*) based on N50, total number of contigs, largest contig, and total length (table S16). MEGAHIT with Kmer length 141 (table S16) produced the best assembly and was therefore used in the downstream analysis. Contigs shorter than 500 bp were removed and ORFs/genes were predicted with Prodigal v2.6.3 (*118*). The primary aim of this study was to identify prokaryotic functional signatures associated with the coral phenotypes, and, therefore, our pipelines focused on identifying prokaryotic genes. As a consequence, eukaryotic ORFs may be underrepresented in our dataset. Future studies using larger sequencing efforts and fractionation methods will be necessary to provide a more comprehensive assessment of both prokaryotic and eukaryotic diversity.

Gene abundance in each metagenome was estimated using Salmon v0.7.2 (*119*). Salmon abundance estimates were used to calculate gene-level offsets using tximport to correct for changes in average gene length across samples (*120*). Taxonomic annotation of ORFs was done using Kaiju v1.7.3 (*121*) using the minimum exact matches mode with a word length of 11 using the nr_euk database. The nr_euk database is prebuilt by Kaiju and contains NCBI nr data from archaea, bacteria, viruses, and microbial eukaryotes (the complete taxa list is available at https://github.com/bioinformatics-centre/kaiju/blob/master/util/kaiju-taxonlistEuk.tsv. Functional annotation against the Kyoto Encyclopedia of Genes and Genomes (KEGG) database was performed using KOfamscan v.1.3.0 (*122*) considering only *e* values <0.001 and bit scores >100. The Shannon diversity index was used to calculate alpha diversity from a rarefied abundances matrix of taxonomic families to a sample count of 95,860 using the Rarefy function from the GUniFrac v1.7 package (*110*). Linear models were fit to test for differences in alpha diversity between phenotypes and time points with the formula Shannon~phenotype*time using the lm function of the stats v4.2 package. Eta-squared values were calculated for linear models to indicate the partial association of each term in the multivariate linear model using the EtaSq function of the DescTools R package. Residuals were tested for normality using the Shapiro-Wilk normality test (W = 0.93, *P* value = 0.14). Pairwise comparisons were conducted using the emmeans package v1.8.2 (*111*). Beta diversity of taxonomic families and KOs counts were estimated using Euclidean distances of centered-log ratio (clr)–transformed gene-level offset matrix using PERMANOVA as described for 16*S* rRNA and ITS2 amplicon data. Differentially abundant taxonomic families and KOs between coral phenotypes and time points were identified using ANCOM-BC v.1.0.2 with FDR-adjusted *P* values <0.05. Given our focus on microbial function, genes not classified as bacteria, archaea, viruses, or microbial eukaryotes were categorized as "unclassified" (likely originating from the coral host). We retained this category in our analysis to prevent uneven alterations in the overall metagenomic composition across samples as suggested previously (*123*, *124*).

In addition, metagenomic binning was conducted by mapping trimmed reads to the metagenomic assembly using Bowtie2 v2.4.1 (*125*). The resulting mapping files were then processed with Metabat2 v2.11.1 (*126*) to calculate tetranucleotide frequencies and differential contig coverage. The quality of the resulting bins was assessed using CheckM v1.1.2 (*127*), with bins meeting the criteria of >75% completeness and <10% contamination classified as metagenome-assembled genomes (MAGs). However, as this approach yielded only two near-complete MAGs (table S17), we opted to exclude them from downstream analysis.

The proportion of unclassified reads was kept in all tables so that all analyses account for the different annotation rates of genes/taxa. In addition, some functional misannotations generated due to intrinsic chance when annotating functionality based on motifs (i.e., KEGG database) were detected manually and disregarded. More specifically, we acknowledge that automated annotation methods in complex datasets with diverse gene origins can result in potential misclassifications. To mitigate this, we manually reviewed the DA

data and excluded genes showing clear inconsistencies, such as eukaryotic genes annotated as bacterial proteins.

Supplementary Materials

The PDF file includes:
Supplementary Material
Figs. S1 to S5
Tables S1 to S8 and S10 to S17
Legend for table S9

Other Supplementary Material for this manuscript includes the following:
Table S9

REFERENCES AND NOTES

1. R. Fisher, R. A. O'Leary, S. Low-Choy, K. Mengersen, N. Knowlton, R. E. Brainard, M. J. Caley, Species richness on coral reefs and the pursuit of convergent global estimates. *Curr. Biol.* **25**, 500–505 (2015).
2. N. Knowlton, E. Corcoran, T. Felis, J. de Goeij, A. Grottoli, Rebuilding coral reefs: A decadal grand challenge (International Coral Reef Society and Future Earth Coasts, 2021); https://doi.org/10.53642/NRKY9386.
3. J. R. Zaneveld, D. E. Burkepile, A. A. Shantz, C. E. Pritchard, R. McMinds, J. P. Payet, R. Welsh, A. M. S. Correa, N. P. Lemoine, S. Rosales, C. Fuchs, J. A. Maynard, R. V. Thurber, Overfishing and nutrient pollution interact with temperature to disrupt coral reefs down to microbial scales. *Nat. Commun.* **7**, 11833 (2016).
4. T. P. Hughes, K. D. Anderson, S. R. Connolly, S. F. Heron, J. T. Kerry, J. M. Lough, A. H. Baird, J. K. Baum, M. L. Berumen, T. C. Bridge, D. C. Claar, C. M. Eakin, J. P. Gilmour, N. A. J. Graham, H. Harrison, J.-P. A. Hobbs, A. S. Hoey, M. Hoogenboom, R. J. Lowe, M. T. McCulloch, J. M. Pandolfi, M. Pratchett, V. Schoepf, G. Torda, S. K. Wilson, Spatial and temporal patterns of mass bleaching of corals in the Anthropocene. *Science* **359**, 80–83 (2018).
5. T. P. Hughes, J. T. Kerry, A. H. Baird, S. R. Connolly, A. Dietzel, C. M. Eakin, S. F. Heron, A. S. Hoey, M. O. Hoogenboom, G. Liu, M. J. McWilliam, R. J. Pears, M. S. Pratchett, W. J. Skirving, J. S. Stella, G. Torda, Global warming transforms coral reef assemblages. *Nature* **556**, 492–496 (2018).
6. G. A. S. Duarte, H. D. M. Villela, M. Deocleciano, D. Silva, A. Barno, P. M. Cardoso, C. L. S. Vilela, P. Rosado, C. S. M. A. Messias, M. A. Chacon, E. P. Santoro, D. B. Olmedo, M. Szpilman, L. A. Rocha, M. Sweet, R. S. Peixoto, Heat waves are a major threat to turbid coral reefs in Brazil. *Front. Mar. Sci.* **7**, 179 (2020).
7. D. J. Barshis, J. T. Ladner, T. A. Oliver, F. O. Seneca, N. Traylor-Knowles, S. R. Palumbi, Genomic basis for coral resilience to climate change. *Proc. Natl. Acad. Sci. U.S.A.* **110**, 1387–1392 (2013).
8. S. R. Palumbi, D. J. Barshis, N. Traylor-Knowles, R. A. Bay, Mechanisms of reef coral resistance to future climate change. *Science* **344**, 895–898 (2014).
9. G. B. Dixon, S. W. Davies, G. V. Aglyamova, E. Meyer, L. K. Bay, M. V. Matz, Genomic determinants of coral heat tolerance across latitudes. *Science* **348**, 1460–1462 (2015).
10. S. B. Matsuda, A. S. Huffmyer, E. A. Lenz, J. M. Davidson, J. R. Hancock, A. Przybylowski, T. Innis, R. D. Gates, K. L. Barott, Coral bleaching susceptibility is predictive of subsequent mortality within but not between coral species. *Front. Ecol. Evol.* **8**, 178 (2020).
11. R. D. H. Barrett, D. Schluter, Adaptation from standing genetic variation. *Trends Ecol. Evol.* **23**, 38–44 (2008).
12. J. A. Fordyce, The evolutionary consequences of ecological interactions mediated through phenotypic plasticity. *J. Exp. Biol.* **209**, 2377–2383 (2006).
13. L. Thomas, N. H. Rose, R. A. Bay, E. H. López, M. K. Morikawa, L. Ruiz-Jones, S. R. Palumbi, Mechanisms of thermal tolerance in reef-building corals across a fine-grained environmental mosaic: Lessons from Ofu, American Samoa. *Front. Mar. Sci.* **4**, 434 (2018).
14. D. J. Barshis, J. H. Stillman, R. D. Gates, R. J. Toonen, L. W. Smith, C. Birkeland, Protein expression and genetic structure of the coral Porites lobata in an environmentally extreme Samoan back reef: Does host genotype limit phenotypic plasticity? *Mol. Ecol.* **19**, 1705–1720 (2010).
15. A. J. Bellantuono, C. Granados-Cifuentes, D. J. Miller, O. Hoegh-Guldberg, M. Rodriguez-Lanetty, Coral thermal tolerance: Tuning gene expression to resist thermal stress. *PLOS ONE* **7**, e50685 (2012).
16. C. Drury, J. Dilworth, E. Majerová, C. Caruso, J. B. Greer, Expression plasticity regulates intraspecific variation in the acclimatization potential of a reef-building coral. *Nat. Commun.* **13**, 4790 (2022).
17. R. Berkelmans, M. J. H. van Oppen, The role of zooxanthellae in the thermal tolerance of corals: A 'nugget of hope' for coral reefs in an era of climate change. *Proc. R. Soc. B* **273**, 2305–2312 (2006).
18. B. C. C. Hume, C. D'Angelo, E. G. Smith, J. R. Stevens, J. Burt, J. Wiedenmann, *Symbiodinium thermophilum* sp. nov., a thermotolerant symbiotic alga prevalent in corals of the world's hottest sea, the Persian/Arabian Gulf. *Sci. Rep.* **5**, 8562 (2015).
19. M. Ziegler, F. O. Seneca, L. K. Yum, S. R. Palumbi, C. R. Voolstra, Bacterial community dynamics are linked to patterns of coral heat tolerance. *Nat. Commun.* **8**, 14213 (2017).
20. E. O. Osman, D. J. Suggett, C. R. Voolstra, D. T. Pettay, D. R. Clark, C. Pogoreutz, E. M. Sampayo, M. E. Warner, D. J. Smith, Coral microbiome composition along the northern Red Sea suggests high plasticity of bacterial and specificity of endosymbiotic dinoflagellate communities. *Microbiome* **8**, 8 (2020).
21. R. Cunning, R. Ritson-Williams, R. D. Gates, Patterns of bleaching and recovery of Montipora capitata in Kāne'ohe Bay, Hawai'i, USA. *Mar. Ecol. Prog. Ser.* **551**, 131–139 (2016).
22. C. R. Voolstra, M. Ziegler, Adapting with microbial help: Microbiome flexibility facilitates rapid responses to environmental change. *Bioessays* **42**, e2000004 (2020).
23. J. Dilworth, C. Caruso, V. A. Kahkejian, A. C. Baker, C. Drury, Host genotype and stable differences in algal symbiont communities explain patterns of thermal stress response of Montipora capitata following thermal pre-exposure and across multiple bleaching events. *Coral Reefs* **40**, 151–163 (2021).
24. Y. Cohen, F. Joseph Pollock, E. Rosenberg, D. G. Bourne, Phage therapy treatment of the coral pathogen Vibrio coralliilyticus. *Microbiology* **2**, 64–74 (2013).
25. L. F. Messer, D. G. Bourne, S. J. Robbins, M. Clay, S. C. Bell, S. J. McIlroy, G. W. Tyson, A genome-centric view of the role of the Acropora kenti microbiome in coral health and resilience. *Nat. Commun.* **15**, 2902 (2024).
26. D. C. A. Leite, J. F. Salles, E. N. Calderon, C. B. Castro, A. Bianchini, J. A. Marques, J. D. van Elsas, R. S. Peixoto, Coral bacterial-core abundance and network complexity as proxies for anthropogenic pollution. *Front. Microbiol.* **9**, 833 (2018).
27. E. P. Santoro, R. M. Borges, J. L. Espinoza, M. Freire, C. S. M. A. Messias, H. D. M. Villela, L. M. Pereira, C. L. S. Vilela, J. G. Rosado, P. M. Cardoso, P. M. Rosado, J. M. Assis, G. A. S. Duarte, G. Perna, A. S. Rosado, A. Macrae, C. L. Dupont, K. E. Nelson, M. J. Sweet, C. R. Voolstra, R. S. Peixoto, Coral microbiome manipulation elicits metabolic and genetic restructuring to mitigate heat stress and evade mortality. *Sci. Adv.* **7**, eabg3088 (2021).
28. P. M. Rosado, D. C. A. Leite, G. A. S. Duarte, R. M. Chaloub, G. Jospin, U. Nunes da Rocha, J. P. Saraiva, F. Dini-Andreote, J. A. Eisen, D. G. Bourne, R. S. Peixoto, Marine probiotics: Increasing coral resistance to bleaching through microbiome manipulation. *ISME J.* **13**, 921–936 (2019).
29. M. Ziegler, C. G. B. Grupstra, M. M. Barreto, M. Eaton, J. BaOmar, K. Zubier, A. Al-Sofyani, A. J. Turki, R. Ormond, C. R. Voolstra, Coral bacterial community structure responds to environmental change in a host-specific manner. *Nat. Commun.* **10**, 3092 (2019).
30. C. A. Lawson, M. Possell, J. R. Seymour, J.-B. Raina, D. J. Suggett, Coral endosymbionts (Symbiodiniaceae) emit species-specific volatilomes that shift when exposed to thermal stress. *Sci. Rep.* **9**, 17395 (2019).
31. L. J. Hill, C. S. M. de Aguiar Messias, C. L. S. Vilela, A. N. Garritano, H. D. M. Villela, F. L. do Carmo, T. Thomas, R. S. Peixoto, Bacteria associated with the in hospite Symbiodiniaceae's phycosphere. *iScience* **27**, 109531 (2024).
32. A. R. Barno, H. D. M. Villela, M. Aranda, T. Thomas, R. S. Peixoto, Host under epigenetic control: A novel perspective on the interaction between microorganisms and corals. *Bioessays* **43**, e2100068 (2021).
33. M. Sweet, H. Villela, T. Keller-Costa, R. Costa, S. Romano, D. G. Bourne, A. Cárdenas, M. J. Huggett, A. H. Kerwin, F. Kuek, M. Medina, J. L. Meyer, M. Müller, F. J. Pollock, M. S. Rappé, M. Sere, K. H. Sharp, C. R. Voolstra, N. Zaccardi, M. Ziegler, R. Peixoto, Insights into the cultured bacterial fraction of corals. *mSystems* **6**, e0124920 (2021).
34. C. R. Voolstra, J.-B. Raina, M. Dörr, A. Cárdenas, C. Pogoreutz, C. B. Silveira, A. R. Mohamed, D. G. Bourne, H. Luo, S. A. Amin, R. S. Peixoto, The coral microbiome in sickness, in health and in a changing world. *Nat. Rev. Microbiol.* **22**, 460–475 (2024).
35. R. S. Peixoto, P. M. Rosado, D. C. de Assis Leite, A. S. Rosado, D. G. Bourne, Beneficial microorganisms for orals (BMC): Proposed mechanisms for coral health and resilience. *Front. Microbiol.* **8**, 341 (2017).
36. F. L. do Carmo, H. F. dos Santos, E. F. Martins, J. D. van Elsas, A. S. Rosado, R. S. Peixoto, Bacterial structure and characterization of plant growth promoting and oil degrading bacteria from the rhizospheres of mangrove plants. *J. Microbiol.* **49**, 535–543 (2011).
37. R. S. Peixoto, C. R. Voolstra, M. Sweet, C. M. Duarte, S. Carvalho, H. Villela, J. E. Lunshof, L. Gram, D. C. Woodhams, J. Walter, A. Roik, U. Hentschel, R. V. Thurber, B. Daisley, B. Ushijima, D. Daffonchio, R. Costa, T. Keller-Costa, J. S. Bowman, A. S. Rosado, G. Reid, C. E. Mason, J. B. Walke, T. Thomas, G. Berg, Harnessing the microbiome to prevent global biodiversity loss. *Nat. Microbiol.* **7**, 1726–1735 (2022).
38. U. E. Siebeck, N. J. Marshall, A. Klüter, O. Hoegh-Guldberg, Monitoring coral bleaching using a colour reference card. *Coral Reefs* **25**, 453–460 (2006).
39. S. Takahashi, H. Bauwe, M. Badger, Impairment of the photorespiratory pathway accelerates photoinhibition of photosystem II by suppression of repair but not acceleration of damage processes in Arabidopsis. *Plant Physiol.* **144**, 487–494 (2007).
40. R. A. Bay, S. R. Palumbi, Multilocus adaptation associated with heat resistance in reef-building corals. *Curr. Biol.* **24**, 2952–2956 (2014).

41. O. Hoegh-Guldberg, L. Hughes, S. McIntyre, D. B. Lindenmayer, C. Parmesan, H. P. Possingham, C. D. Thomas, Assisted colonization and rapid climate change. *Science* **321**, 345–346 (2008).
42. R. S. Santos, T. C. LaJeunesse, Searchable database of Symbiodinium diversity—Geographic and ecological diversity (SD2-GED), Auburn University, Auburn, AL (2006).
43. A. W. Silva Lima, L. Leomil, L. Oliveira, T. Varasteh, J. R. Thompson, M. Medina, C. C. Thompson, F. L. Thompson, Insights on the genetic repertoire of the coral Mussismilia braziliensis endosymbiont Symbiodinium. *Symbiosis* **80**, 183–193 (2020).
44. J. M. Reynolds, B. U. Bruns, W. K. Fitt, G. W. Schmidt, Enhanced photoprotection pathways in symbiotic dinoflagellates of shallow-water corals and other cnidarians. *Proc. Natl. Acad. Sci. U.S.A.* **105**, 13674–13678 (2008).
45. A. G. Grottoli, M. E. Warner, S. J. Levas, M. D. Aschaffenburg, V. Schoepf, M. McGinley, J. Baumann, Y. Matsui, The cumulative impact of annual coral bleaching can turn some coral species winners into losers. *Glob. Chang. Biol.* **20**, 3823–3833 (2014).
46. S. E. Gantt, E. F. Keister, A. A. Manfroy, D. E. Merck, W. K. Fitt, E. M. Muller, D. W. Kemp, Wild and nursery-raised corals: Comparative physiology of two framework coral species. *Coral Reefs* **42**, 299–310 (2023).
47. P. Mulo, C. Sicora, E.-M. Aro, Cyanobacterial psbA gene family: Optimization of oxygenic photosynthesis. *Cell. Mol. Life Sci.* **66**, 3697–3710 (2009).
48. M. Suorsa, E.-M. Aro, Expression, assembly and auxiliary functions of photosystem II oxygen-evolving proteins in higher plants. *Photosynth. Res.* **93**, 89–100 (2007).
49. I. Mouyna, L. Hartl, J.-P. Latgé, β-1,3-glucan modifying enzymes in *Aspergillus fumigatus*. *Front. Microbiol.* **4**, 81 (2013).
50. M. de Medina-Redondo, Y. Arnáiz-Pita, T. Fontaine, F. Del Rey, J. P. Latgé, C. R. Vázquez de Aldana, The β-1,3-glucanosyltransferase gas4p is essential for ascospore wall maturation and spore viability in *Schizosaccharomyces pombe*. *Mol. Microbiol.* **68**, 1283–1299 (2008).
51. D. A. Schoenberg, R. K. Trench, Genetic variation in Symbiodinium (= Gymnodinium) *microadriaticum* Freudenthal, and specificity in its symbiosis with marine invertebrates. III. Specificity and inlfectivity of *Symbiodinium microadriaticum*. *Proc. R. Soc. Lond. B* **207**, 445–460 (1980).
52. N. J. Colley, R. K. Trench, Selectivity in phagocytosis and persistence of symbiotic algae in the scyphistoma stage of the jellyfish Cassiopeia xamachana. *Proc. R. Soc. Lond. B Biol. Sci.* **219**, 61–82 (1983).
53. C. Almaguer, W. Cheng, C. Nolder, J. Patton-Vogt, Glycerophosphoinositol, a novel phosphate source whose transport is regulated by multiple factors in Saccharomyces cerevisiae. *J. Biol. Chem.* **279**, 31937–31942 (2004).
54. N. Zein, W. Solomon, K. L. Colson, D. R. Schroeder, Maduropeptin: An antitumor chromoprotein with selective protease activity and DNA cleaving properties. *Biochemistry* **34**, 11591–11597 (1995).
55. N. J. Bauer, A. J. Kreuzman, J. E. Dotzlaf, W. K. Yeh, Purification, characterization, and kinetic mechanism of S-adenosyl-L-methionine:Macrocin O-methyltransferase from Streptomyces fradiae. *J. Biol. Chem.* **263**, 15619–15625 (1988).
56. E. C. E. Kvennefors, E. Sampayo, C. Kerr, G. Vieira, G. Roff, A. C. Barnes, Regulation of bacterial communities through antimicrobial activity by the coral holobiont. *Microb. Ecol.* **63**, 605–618 (2012).
57. S. A. Amin, M. S. Parker, E. V. Armbrust, Interactions between diatoms and bacteria. *Microbiol. Mol. Biol. Rev.* **76**, 667–684 (2012).
58. A. A. Shibl, A. Isaac, M. A. Ochsenkühn, A. Cárdenas, C. Fei, G. Behringer, M. Arnoux, N. Drou, M. P. Santos, K. C. Gunsalus, C. R. Voolstra, S. A. Amin, Diatom modulation of select bacteria through use of two unique secondary metabolites. *Proc. Natl. Acad. Sci. U.S.A.* **117**, 27445–27455 (2020).
59. J. C. Frommlet, M. L. Sousa, A. Alves, S. I. Vieira, D. J. Suggett, J. Serôdio, Coral symbiotic algae calcify ex hospite in partnership with bacteria. *Proc. Natl. Acad. Sci. U.S.A.* **112**, 6158–6163 (2015).
60. J. Maire, S. K. Girvan, S. E. Barkla, A. Perez-Gonzalez, D. J. Suggett, L. L. Blackall, M. J. H. van Oppen, Intracellular bacteria are common and taxonomically diverse in cultured and in hospite algal endosymbionts of coral reefs. *ISME J.* **15**, 2028–2042 (2021).
61. W. Bell, R. Mitchell, Chemotactic and growth responses of marine bacteria to algal extracellular products. *Biol. Bull.* **143**, 265–277 (1972).
62. A. G. Garrido, L. F. Machado, C. Zilberberg, D. C. de Assis Leite, Insights into 'Symbiodiniaceae phycosphere' in a coral holobiont. *Symbiosis* **83**, 25–39 (2021).
63. T. C. LaJeunesse, J. E. Parkinson, P. W. Gabrielson, H. J. Jeong, J. D. Reimer, C. R. Voolstra, S. R. Santos, Systematic revision of symbiodiniaceae highlights the antiquity and diversity of coral endosymbionts. *Curr. Biol.* **28**, 2570–2580.e6 (2018).
64. A. Kazaks, T. Voronkova, J. Rumnieks, A. Dishlers, K. Tars, Genome structure of caulobacter phage phiCb5. *J. Virol.* **85**, 4628–4631 (2011).
65. E. P. Starr, E. E. Nuccio, J. Pett-Ridge, J. F. Banfield, M. K. Firestone, Metatranscriptomic reconstruction reveals RNA viruses with the potential to shape carbon cycling in soil. *Proc. Natl. Acad. Sci. U.S.A.* **116**, 25900–25908 (2019).
66. S. R. Krishnamurthy, A. B. Janowski, G. Zhao, D. Barouch, D. Wang, Hyperexpansion of RNA bacteriophage diversity. *PLOS Biol.* **14**, e1002409 (2016).
67. A. Cárdenas, J. Ye, M. Ziegler, J. P. Payet, R. McMinds, R. Vega Thurber, C. R. Voolstra, Coral-associated viral assemblages from the central Red Sea align with host species and contribute to holobiont genetic diversity. *Front. Microbiol.* **11**, 572534 (2020).
68. M. Nassal, Hepatitis B viruses: Reverse transcription a different way. *Virus Res.* **134**, 235–249 (2008).
69. T. Coral, M. Descostes, H. De Boissezon, R. Bernier-Latmani, L. F. de Alencastro, P. Rossi, Microbial communities associated with uranium in-situ recovery mining process are related to acid mine drainage assemblages. *Sci. Total Environ.* **628-629**, 26–35 (2018).
70. E. St John, A.-L. Reysenbach, Genomic comparison of deep-sea hydrothermal genera related to *Aeropyrum*, *Thermodiscus* and *Caldisphaera*, and proposed emended description of the family Acidilobaceae. *Syst. Appl. Microbiol.* **47**, 126507 (2024).
71. M. Kerou, C. Schleper, Nitrososphaeraceae, *Bergey's Manual of Systematics of Archaea and Bacteria* (2016), pp. 1–2; DOI: 10.1002/9781118960608.
72. S. M. Rosales, L. K. Huebner, J. S. Evans, A. Apprill, A. C. Baker, C. C. Becker, A. J. Bellantuono, M. E. Brandt, A. S. Clark, J. Del Campo, C. E. Dennison, K. R. Eaton, N. E. Huntley, C. A. Kellogg, M. Medina, J. L. Meyer, E. M. Muller, M. Rodriguez-Lanetty, J. L. Salerno, W. B. Schill, E. N. Shilling, J. M. Stewart, J. D. Voss, A meta-analysis of the stony coral tissue loss disease microbiome finds key bacteria in unaffected and lesion tissue in diseased colonies. *ISME Commun.* **3**, 19 (2023).
73. C. J. Krediet, K. B. Ritchie, V. J. Paul, M. Teplitski, Coral-associated micro-organisms and their roles in promoting coral health and thwarting diseases. *Proc. R. Soc. B* **280**, 20122328 (2013).
74. R. Vega Thurber, L. D. Mydlarz, M. Brandt, D. Harvell, E. Weil, L. Raymundo, B. L. Willis, S. Langevin, A. M. Tracy, R. Littman, K. M. Kemp, P. Dawkins, K. C. Prager, M. Garren, J. Lamb, Deciphering coral disease dynamics: Integrating host, microbiome, and the changing environment. *Front. Ecol. Evol.* **8**, 575927 (2020).
75. H. Mera, D. G. Bourne, Disentangling causation: Complex roles of coral-associated microorganisms in disease. *Environ. Microbiol.* **20**, 431–449 (2018).
76. A. Erlacher, T. Cernava, M. Cardinale, J. Soh, C. W. Sensen, M. Grube, G. Berg, *Rhizobiales* as functional and endosymbiontic members in the lichen symbiosis of *Lobaria pulmonaria L*. *Front. Microbiol.* **6**, 53 (2015).
77. R. Garrido-Oter, R. T. Nakano, N. Dombrowski, K.-W. Ma, The AgBiome Team, A. C. McHardy, P. Schulze-Lefert, Modular traits of the Rhizobiales root microbiota and their evolutionary relationship with symbiotic rhizobia. *Cell Host Microbe* **24**, 155–167.e5 (2018).
78. B. D. Young, S. M. Rosales, I. C. Enochs, G. Kolodziej, N. Formel, A. Moura, G. L. D'Alonso, N. Traylor-Knowles, Different disease inoculations cause common responses of the host immune system and prokaryotic component of the microbiome in *Acropora palmata*. *PLOS ONE* **18**, e0286293 (2023).
79. T. G. Lilburn, K. S. Kim, N. E. Ostrom, K. R. Byzek, J. R. Leadbetter, J. A. Breznak, Nitrogen fixation by symbiotic and free-living spirochetes. *Science* **292**, 2495–2498 (2001).
80. B. J. Baker, C. S. Lazar, A. P. Teske, G. J. Dick, Genomic resolution of linkages in carbon, nitrogen, and sulfur cycling among widespread estuary sediment bacteria. *Microbiome* **3**, 14 (2015).
81. J. Hernández-Zulueta, L. Díaz-Pérez, A. Echeverría-Vega, G. G. Nava-Martínez, M. Á. García-Salgado, F. A. Rodríguez-Zaragoza, An update of knowledge of the bacterial assemblages associated with the mexican caribbean corals *Acropora palmata*, *Orbicella faveolata*, and *Porites porites*. *Diversity* **15**, 964 (2023).
82. J. A. J. M. van de Water, D. Allemand, C. Ferrier-Pagès, Bacterial symbionts of the precious coral *Corallium rubrum* are differentially distributed across colony-specific compartments and differ among colormorphs. *Environ. Microbiol. Rep.* **16**, e13236 (2024).
83. E. M. Díaz-Almeyda, T. Ryba, A. H. Ohdera, S. M. Collins, N. Shafer, C. Link, M. Prado-Zapata, C. Ruhnke, M. Moore, A. M. González Angel, F. J. Pollock, M. Medina, Thermal stress has minimal effects on bacterial communities of thermotolerant Symbiodinium cultures. *Front. Ecol. Evol.* **10**, 764086 (2022).
84. T. Keller-Costa, D. Eriksson, J. M. S. Gonçalves, N. C. M. Gomes, A. Lago-Lestón, R. Costa, The gorgonian coral *Eunicella labiata* hosts a distinct prokaryotic consortium amenable to cultivation. *FEMS Microbiol. Ecol.* **93**, fix143 (2017).
85. S. G. Silva, A. Lago-Lestón, R. Costa, T. Keller-Costa, Draft genome sequence of *Sphingorhabdus* sp. Strain EL138, a metabolically versatile alphaproteobacterium isolated from the gorgonian coral *Eunicella labiata*. *Genome Announc.* **6**, 10.1128/genomea.00142-18 (2018).
86. M. Ziegler, A. Roik, A. Porter, K. Zubier, M. S. Mudarris, R. Ormond, C. R. Voolstra, Coral microbial community dynamics in response to anthropogenic impacts near a major city in the central Red Sea. *Mar. Pollut. Bull.* **105**, 629–640 (2016).
87. M. G. Séré, P. Tortosa, P. Chabanet, J. Turquet, J.-P. Quod, M. H. Schleyer, Bacterial communities associated with *Porites* white patch syndrome (PWPS) on three western Indian Ocean (WIO) coral reefs. *PLOS ONE* **8**, e83746 (2013).
88. C. Roder, C. Arif, T. Bayer, M. Aranda, C. Daniels, A. Shibl, S. Chavanich, C. R. Voolstra, Bacterial profiling of white plague disease in a comparative coral species framework. *ISME J.* **8**, 31–39 (2014).

89. L. J. Baker, H. G. Reich, S. A. Kitchen, J. G. Klinges, H. R. Koch, I. B. Baums, E. M. Muller, R. V. Thurber, The coral symbiont *Candidatus* Aquarickettsia is variably abundant in threatened Caribbean acroporids and transmitted horizontally. *ISME J.* **16**, 400–411 (2022).
90. D. B. Antonio, K. B. Andree, J. D. Moore, C. S. Friedman, R. P. Hedrick, Detection of Rickettsiales-like prokaryotes by in situ hybridization in black abalone, *Haliotis cracherodii*, with withering syndrome. *J. Invertebr. Pathol.* **75**, 180–182 (2000).
91. C. Kebbi-Beghdadi, C. Batista, G. Greub, Permissivity of fish cell lines to three *Chlamydia*-related bacteria: *Waddlia chondrophila*, *Estrella lausannensis* and *Parachlamydia acanthamoebae*. *FEMS Immunol. Med. Microbiol.* **63**, 339–345 (2011).
92. S. M. Rosales, L. K. Huebner, A. S. Clark, R. McMinds, R. R. Ruzicka, E. M. Muller, Bacterial metabolic potential and micro-eukaryotes enriched in stony coral tissue loss disease lesions. *Front. Mar. Sci.* **8**, 10.3389/fmars.2021.776859 (2022).
93. S. Louca, M. F. Polz, F. Mazel, M. B. N. Albright, J. A. Huber, M. I. O'Connor, M. Ackermann, A. S. Hahn, D. S. Srivastava, S. A. Crowe, M. Doebeli, L. W. Parfrey, Function and functional redundancy in microbial systems. *Nat. Ecol. Evol.* **2**, 936–943 (2018).
94. A. Cárdenas, J.-B. Raina, C. Pogoreutz, N. Rädecker, J. Bougoure, P. Guagliardo, M. Pernice, C. R. Voolstra, Greater functional diversity and redundancy of coral endolithic microbiomes align with lower coral bleaching susceptibility. *ISME J.* **16**, 2406–2420 (2022).
95. C. D. Teixeira, R. L. L. Leitão, F. V. Ribeiro, F. C. Moraes, L. M. Neves, A. C. Bastos, G. H. Pereira-Filho, M. Kampel, P. S. Salomon, J. A. Sá, L. N. Falsarella, M. Amario, M. L. Abieri, R. C. Pereira, G. M. Amado-Filho, R. L. Moura, Sustained mass coral bleaching (2016–2017) in Brazilian turbid-zone reefs: Taxonomic, cross-shelf and habitat-related trends. *Coral Reefs* **38**, 801–813 (2019).
96. C. R. Voolstra, K. M. Quigley, S. W. Davies, J. E. Parkinson, R. S. Peixoto, M. Aranda, A. C. Baker, A. R. Barno, D. J. Barshis, F. Benzoni, V. Bonito, D. G. Bourne, C. Buitrago-López, T. C. L. Bridge, C. X. Chan, D. J. Combosch, J. Craggs, J. C. Frommlet, S. Herrera, A. M. Quattrini, T. Röthig, J. D. Reimer, E. Rubio-Portillo, D. J. Suggett, H. Villela, M. Ziegler, M. Sweet, Consensus guidelines for advancing coral holobiont genome and specimen voucher deposition. *Front. Mar. Sci.* **8**, 701784 (2021).
97. A. G. Grottoli, R. J. Toonen, R. van Woesik, R. Vega Thurber, M. E. Warner, R. H. McLachlan, J. T. Price, K. D. Bahr, I. B. Baums, K. D. Castillo, M. A. Coffroth, R. Cunning, K. L. Dobson, M. J. Donahue, J. L. Hench, R. Iglesias-Prieto, D. W. Kemp, C. D. Kenkel, D. I. Kline, I. B. Kuffner, J. L. Matthews, A. B. Mayfield, J. L. Padilla-Gamiño, S. Palumbi, C. R. Voolstra, V. M. Weis, H. C. Wu, Increasing comparability among coral bleaching experiments. *Ecol. Appl.* **31**, e02262 (2021).
98. K. M. Horvath, K. D. Castillo, P. Armstrong, I. T. Westfield, T. Courtney, J. B. Ries, Next-century ocean acidification and warming both reduce calcification rate, but only acidification alters skeletal morphology of reef-building coral *Siderastrea siderea*. *Sci. Rep.* **6**, 29613 (2016).
99. D. Bates, M. Mächler, B. Bolker, S. Walker, Fitting linear mixed-effects models using lme4, arXiv:1406.5823 [stat.CO] (2014). http://arxiv.org/abs/1406.5823.
100. B. C. C. Hume, M. Ziegler, J. Poulain, X. Pochon, S. Romac, E. Boissin, C. de Vargas, S. Planes, P. Wincker, C. R. Voolstra, An improved primer set and amplification protocol with increased specificity and sensitivity targeting the *Symbiodinium* ITS2 region. *PeerJ* **6**, e4816 (2018).
101. J. G. Caporaso, C. L. Lauber, W. A. Walters, D. Berg-Lyons, C. A. Lozupone, P. J. Turnbaugh, N. Fierer, R. Knight, Global patterns of 16S rRNA diversity at a depth of millions of sequences per sample. *Proc. Natl. Acad. Sci. U.S.A.* **108**, 4516–4522 (2011).
102. B. C. C. Hume, E. G. Smith, M. Ziegler, H. J. M. Warrington, J. A. Burt, T. C. LaJeunesse, J. Wiedenmann, C. R. Voolstra, SymPortal: A novel analytical framework and platform for coral algal symbiont next-generation sequencing *ITS2* profiling. *Mol. Ecol. Resour.* **19**, 1063–1080 (2019).
103. P. D. Schloss, S. L. Westcott, T. Ryabin, J. R. Hall, M. Hartmann, E. B. Hollister, R. A. Lesniewski, B. B. Oakley, D. H. Parks, C. J. Robinson, J. W. Sahl, B. Stres, G. G. Thallinger, D. J. Van Horn, C. F. Weber, Introducing mothur: Open-source, platform-independent, community-supported software for describing and comparing microbial communities. *Appl. Environ. Microbiol.* **75**, 7537–7541 (2009).
104. C. Camacho, G. Coulouris, V. Avagyan, N. Ma, J. Papadopoulos, K. Bealer, T. L. Madden, BLAST$_+$: Architecture and applications. *BMC Bioinformatics* **10**, 421 (2009).
105. A. M. Eren, H. G. Morrison, P. J. Lescault, J. Reveillaud, J. H. Vineis, M. L. Sogin, Minimum entropy decomposition: Unsupervised oligotyping for sensitive partitioning of high-throughput marker gene sequences. *ISME J.* **9**, 968–979 (2015).
106. B. J. Callahan, P. J. McMurdie, M. J. Rosen, A. W. Han, A. J. A. Johnson, S. P. Holmes, DADA2: High-resolution sample inference from Illumina amplicon data. *Nat. Methods* **13**, 581–583 (2016).
107. C. Quast, E. Pruesse, P. Yilmaz, J. Gerken, T. Schweer, P. Yarza, J. Peplies, F. O. Glöckner, The SILVA ribosomal RNA gene database project: Improved data processing and web-based tools. *Nucleic Acids Res.* **41**, D590–D596 (2013).
108. P. J. McMurdie, S. Holmes, phyloseq: An R package for reproducible interactive analysis and graphics of microbiome census data. *PLOS ONE* **8**, e61217 (2013).
109. P. Dixon, VEGAN, a package of R functions for community ecology. *J. Veg. Sci.* **14**, 927–930 (2003).
110. J. Chen, X. Zhang, L. Yang, M. J. Chen, Package GUniFrac (2022). http://cran.uni-muenster.de/web/packages/GUniFrac/GUniFrac.pdf.
111. S. R. Searle, F. M. Speed, G. A. Milliken, Population marginal means in the linear model: An alternative to least squares means. *Am. Stat.* **34**, 216–221 (1980).
112. H. Lin, S. D. Peddada, Analysis of compositions of microbiomes with bias correction. *Nat. Commun.* **11**, 3514 (2020).
113. A. M. Bolger, M. Lohse, B. Usadel, Trimmomatic: A flexible trimmer for Illumina sequence data. *Bioinformatics* **30**, 2114–2120 (2014).
114. D. Li, R. Luo, C.-M. Liu, C.-M. Leung, H.-F. Ting, K. Sadakane, H. Yamashita, T.-W. Lam, MEGAHIT v1.0: A fast and scalable metagenome assembler driven by advanced methodologies and community practices. *Methods* **102**, 3–11 (2016).
115. A. Prjibelski, D. Antipov, D. Meleshko, A. Lapidus, A. Korobeynikov, Using SPAdes de novo assembler. *Curr. Protoc. Bioinformatics* **70**, e102 (2020).
116. Y. Peng, H. C. M. Leung, S. M. Yiu, F. Y. L. Chin, Meta-IDBA: A de novo assembler for metagenomic data. *Bioinformatics* **27**, i94–i101 (2011).
117. A. Gurevich, V. Saveliev, N. Vyahhi, G. Tesler, QUAST: Quality assessment tool for genome assemblies. *Bioinformatics* **29**, 1072–1075 (2013).
118. D. Hyatt, G.-L. Chen, P. F. LoCascio, M. L. Land, F. W. Larimer, L. J. Hauser, Prodigal: Prokaryotic gene recognition and translation initiation site identification. *BMC Bioinformatics* **11**, 119 (2010).
119. R. Patro, G. Duggal, M. I. Love, R. A. Irizarry, C. Kingsford, Salmon provides fast and bias-aware quantification of transcript expression. *Nat. Methods* **14**, 417–419 (2017).
120. C. Soneson, M. I. Love, M. D. Robinson, Differential analyses for RNA-seq: Transcript-level estimates improve gene-level inferences. *F1000Res* **4**, 1521 (2015).
121. P. Menzel, K. L. Ng, A. Krogh, Fast and sensitive taxonomic classification for metagenomics with Kaiju. *Nat. Commun.* **7**, 11257 (2016).
122. T. Aramaki, R. Blanc-Mathieu, H. Endo, K. Ohkubo, M. Kanehisa, S. Goto, H. Ogata, KofamKOALA: KEGG ortholog assignment based on profile HMM and adaptive score threshold. *Bioinformatics* **36**, 2251–2252 (2020).
123. S. Nayfach, K. S. Pollard, Toward accurate and quantitative comparative metagenomics. *Cell* **166**, 1103–1116 (2016).
124. L. C. Xia, J. A. Cram, T. Chen, J. A. Fuhrman, F. Sun, Accurate genome relative abundance estimation based on shotgun metagenomic reads. *PLOS ONE* **6**, e27992 (2011).
125. B. Langmead, S. L. Salzberg, Fast gapped-read alignment with Bowtie 2. *Nat. Methods* **9**, 357–359 (2012).
126. D. D. Kang, F. Li, E. Kirton, A. Thomas, R. Egan, H. An, Z. Wang, MetaBAT 2: An adaptive binning algorithm for robust and efficient genome reconstruction from metagenome assemblies. *PeerJ* **7**, e7359 (2019).
127. D. H. Parks, M. Imelfort, C. T. Skennerton, P. Hugenholtz, G. W. Tyson, CheckM: Assessing the quality of microbial genomes recovered from isolates, single cells, and metagenomes. *Genome Res.* **25**, 1043–1055 (2015).

Acknowledgments: We would like to thank M. Szpilman, R. Franco, P. Spina, and the AquaRio - Marine Aquarium of Rio de Janeiro team for the corals donated to this study and for the support provided during the experiment. We would also like to thank J. Curdia for statistical advice for data analysis. **Funding:** R.S.P. was supported through funding provided by AquaRio and KAUST grant numbers BAS/1/1095-01-01 and FCC/1/1976-40-01.
Author contributions: E.P.S., H.D.M.V., G.A.S.D., and R.S.P. conceived and designed the study. E.P.S., H.D.M.V., C.L.S.V., A.M.G., and G.A.S.D. assembled the mesocosms and performed the experiments. E.P.S., A.C., G.P., and C.R.V. conducted DNA extractions, sequencing, bioinformatics, and statistical analyses. E.P.S., A.C., J.P.S., T.T., R.S.P., and C.R.V. analyzed and interpreted the data. R.S.P. provided financial support. E.P.S., A.C., C.R.V., and R.S.P. wrote the manuscript. All authors were involved in the critical revision of the manuscript. All authors read and approved the final manuscript. **Competing interests:** The authors declare that they have no competing interests. **Data and materials availability:** All data needed to evaluate the conclusions in the paper are present in the paper and/or the Supplementary Materials. 16*S* rRNA gene, ITS2, and metagenome sequences are available at NCBI under the BioProject PRJNA607335. R scripts used for 16*S* rRNA, ITS2, and metagenomic analysis are deposited on Zenodo (10.5281/zenodo.13997232).

Submitted 5 May 2024
Accepted 16 December 2024
Published 17 January 2025
10.1126/sciadv.adq2583